
Near-Minimax-Optimal Distributional Reinforcement Learning with a Generative Model

Mark Rowland¹ Li Kevin Wenliang¹ Rémi Munos¹ Clare Lyle¹ Yunhao Tang¹ Will Dabney¹

Abstract

We propose a new algorithm for model-based distributional reinforcement learning (RL), and prove that it is minimax-optimal for approximating return distributions with a generative model (up to logarithmic factors), resolving an open question of Zhang et al. (2023). Our analysis provides new theoretical results on categorical approaches to distributional RL, and also introduces a new distributional Bellman equation, the stochastic categorical CDF Bellman equation, which we expect to be of independent interest. We also provide an experimental study comparing several model-based distributional RL algorithms, with several takeaways for practitioners.

1. Introduction

In distributional reinforcement learning, the aim is to predict the full probability distribution of possible returns at each state, rather than just the mean return (Morimura et al., 2010a; Bellemare et al., 2017; 2023). Applications of distributional reinforcement learning range from dopamine response modelling in neuroscience (Dabney et al., 2020), to driving risk-sensitive decision-making and exploration in domains such as robotics (Bodnar et al., 2020), healthcare (Böck et al., 2022), and algorithm discovery (Fawzi et al., 2022), as well as forming a core component of many deep reinforcement learning architectures (Bellemare et al., 2017; Dabney et al., 2018b;a; Yang et al., 2019; Bellemare et al., 2020; Shahriari et al., 2022; Wurman et al., 2022).

Beyond asymptotic convergence (Rowland et al., 2018; 2023; Bellemare et al., 2023), an emerging topic in the theory of distributional RL is that of finite-sample bounds (Böck & Heirzinger, 2022; Wu et al., 2023): *How many samples are required to learn accurate return-distribution estimates?*

Zhang et al. (2023) make a variety of contributions in the

¹Google DeepMind. Correspondence to: Mark Rowland <markrowland@google.com>.

Preprint.

setting where samples are obtained via a *generative model*, whereby one can obtain sample transitions at any desired state in the environment, a commonly studied regime for mean-return RL (Kearns et al., 2002; Kakade, 2003; Azar et al., 2013). Zhang et al. (2023) prove a lower bound of $N = \Omega(\varepsilon^{-2}(1-\gamma)^{-3})$ samples required per state in order to obtain ε -accurate return-distribution estimates with high probability, as measured by Wasserstein distance (here, $\gamma \in [0, 1)$ is the discount factor). This matches the minimax sample complexity of learning an accurate value function (Azar et al., 2013). Zhang et al. (2023) also propose an algorithm with a sample complexity bound of $N = \tilde{O}(\varepsilon^{-2}(1-\gamma)^{-4})$ for the problem above.

This leaves two key questions open. First, there is gap of $O((1-\gamma)^{-1})$ between the bounds above: Can the upper bound be improved, or in other words, *is distributional RL statistically harder than learning a value function with a generative model?* Second, the algorithm proposed by Zhang et al. (2023) is typically not implementable in practice, as it involves solving the *unprojected* distributional Bellman equation over an infinite-dimensional space of probability distributions (the authors use approximate methods in their experiments for this reason): *Is there a tractable algorithm that achieves the lower bound?* We resolve both these questions with the following contributions:

- We propose the *direct categorical fixed-point algorithm* (DCFP), a new distributional RL algorithm based on the categorical approach (Bellemare et al., 2017).
- We prove that with an appropriate number of categories, DCFP has a sample complexity of $\tilde{O}(\varepsilon^{-2}(1-\gamma)^{-3})$ (for attaining ε -accurate Wasserstein-1 return-distribution approximations with high probability), matching the minimax lower bound up to logarithmic factors. This shows that in this context, distributional RL is no harder statistically than learning an accurate value function.
- Our analysis introduces a novel distributional RL concept which we expect to be of independent interest: the *stochastic categorical CDF Bellman equation*.
- We also study the empirical performance of several algorithms for distributional RL with a generative model, and identify several key findings for practitioners.

2. Background

Throughout the paper, we consider the problem of evaluation in an infinite-horizon Markov reward process (MRP), with finite state space \mathcal{X} , transition probabilities $P \in \mathbb{R}^{\mathcal{X} \times \mathcal{X}}$, reward function $r : \mathcal{X} \rightarrow [0, 1]$, and discount factor $\gamma \in [0, 1)$. A random trajectory $(X_t, R_t)_{t \geq 0}$ is generated from an initial state $X_0 = x$ according to the conditional distributions $X_t | (X_0, \dots, X_{t-1}) \sim P(\cdot | X_{t-1})$, and $R_t = r(X_t)$. The return associated with the trajectory is given by the quantity $\sum_{t \geq 0} \gamma^t R_t$. In RL, a central task is to estimate the value function $V^* : \mathcal{X} \rightarrow \mathbb{R}$, defined by

$$V^*(x) = \mathbb{E}[\sum_{t \geq 0} \gamma^t R_t | X_0 = x], \quad (1)$$

given some form of observations from the MRP. The value function defines the expected return, conditional on each possible starting state in the MRP.

The value function satisfies the Bellman equation $V^* = TV^*$, where $T : \mathbb{R}^{\mathcal{X}} \rightarrow \mathbb{R}^{\mathcal{X}}$ is defined by

$$(TV)(x) = \mathbb{E}_x[R + \gamma V(X')], \quad (2)$$

where (X, R, X') is a random transition in the environment, distributed as described above. When the transition probabilities of the MRP are known, the right-hand side can be evaluated as an affine transformation of V . MRP theory (see, e.g., Puterman, 2014 for an overview) then provides two methods for obtaining (an approximation to) V^* . First, *dynamic programming* (DP), in which an initial approximation $V_0 \in [0, (1 - \gamma)^{-1}]^{\mathcal{X}}$ is taken, and the sequence $(V_k)_{k=0}^{\infty}$ is computed via the update $V_{k+1} = TV_k$; it is guaranteed that $\|V_k - V^*\|_{\infty} \leq \gamma^k (1 - \gamma)^{-1}$. Second, *direct solution*, in which the linear system $V = TV$ is solved directly to obtain V^* as its unique solution.

2.1. Reinforcement learning with a generative model

In many settings the transition probabilities of the MRP are unknown, and the value function must be estimated based on data comprising sampled transitions, introducing a statistical element to the problem. A commonly used model for this data is a *generative model* (Kearns et al., 2002; Kakade, 2003). In this setting, for each state $x \in \mathcal{X}$, we observe N i.i.d. samples $(X_i^x)_{i=1}^N$ from $P(\cdot | x)$, and this collection of $N|\mathcal{X}|$ samples may then be used by an algorithm to estimate the value function. Azar et al. (2013) showed that at least $N = \Omega(\varepsilon^{-2}(1 - \gamma)^{-3} \log(|\mathcal{X}|/\delta))$ samples are required to obtain ε -accurate estimates of the value function with high probability (measured in L^{∞} norm), and also showed that this bound is attained (up to logarithmic factors) by a *certainty equivalence* algorithm, which treats the empirically observed transition frequencies as the true ones, and solves for the value function of the corresponding MRP.

Mathematically, the algorithm constructs the empirical transition probability matrix $\hat{P} \in \mathbb{R}^{\mathcal{X} \times \mathcal{X}}$, given by $\hat{P}(y|x) =$

$N^{-1} \sum_{i=1}^N \mathbb{1}\{X_i^x = y\}$. From this, the empirical Bellman operator \hat{T} can be defined as in Equation (2), with the expectation now computed with respect to \hat{P} . One then solves the empirical Bellman equation $V = \hat{T}V$ to obtain an estimated value function \hat{V} . Azar et al. (2013) show that for sufficiently small $\varepsilon > 0$ and given $\delta \in (0, 1)$, with $N = \Omega(\varepsilon^{-2}(1 - \gamma)^{-3} \log(|\mathcal{X}|/\delta))$ samples, we have $\|\hat{V} - V^*\|_{\infty} \leq \varepsilon$ with probability at least $1 - \delta$, which matches the lower bound described above.

2.2. Distributional reinforcement learning

Distributional RL aims to capture the full probability distribution of the random return at each state, not just its mean. Mathematically, the object of interest is the return-distribution function (RDF) $\eta^* : \mathcal{X} \rightarrow \mathcal{P}(\mathbb{R})$, defined by

$$\eta^*(x) = \mathcal{D}(\sum_{t=0}^{\infty} \gamma^t R_t | X_0 = x), \quad (3)$$

where \mathcal{D} extracts the probability distribution of the input random variable. The distributional perspective on reinforcement learning has proved practically useful in a wide variety of applications, including healthcare (Böck et al., 2022), navigation (Bellemare et al., 2020), and algorithm discovery (Fawzi et al., 2022).

The central equation behind dynamic programming approaches to approximating the return distribution function is the *distributional Bellman equation* (Sobel, 1982; Morimura et al., 2010a; Bellemare et al., 2017), given by

$$\eta^* = \mathcal{T}\eta^*,$$

where $\mathcal{T} : \mathcal{P}(\mathbb{R})^{\mathcal{X}} \rightarrow \mathcal{P}(\mathbb{R})^{\mathcal{X}}$ is the *distributional Bellman operator*, defined by

$$(\mathcal{T}\eta)(x) = \mathcal{D}(R + \gamma G(X') | X = x),$$

where independent from the random transition (X, R, X') , we have $G(x) \sim \eta(x)$ for each $x \in \mathcal{X}$.

2.3. Categorical dynamic programming

Given an initial RDF approximation $\eta \in \mathcal{P}([0, (1 - \gamma)^{-1}])^{\mathcal{X}}$, it also holds that the update $\eta \leftarrow \mathcal{T}\eta$ converges to η^* in an appropriate sense (e.g., in Wasserstein distance; see Bellemare et al., 2017), in analogy with mean-return DP. However, probability distributions are infinite-dimensional objects, and as such it is rarely the case that this update can actually be implemented and carried out in practice. Instead, the use of some kind of approximate, tractable representation of probability distributions is typically required.

Representations. In this paper, we focus on the categorical approach to distributional reinforcement learning (Bellemare et al., 2017), in which estimates of return distributions are represented as categorical distributions over a finite number of outcomes $z_1 < \dots < z_m$. We will take $\{z_1, \dots, z_m\}$

to be an equally spaced grid over the range of possible returns $[0, (1 - \gamma)^{-1}]$, so that $z_i = \frac{i-1}{m-1}(1 - \gamma)^{-1}$ for $i = 1, \dots, m$. Approximations of the RDF are then represented as $\eta_p : \mathcal{X} \rightarrow \mathcal{P}(\mathbb{R})$, where

$$\eta_p(x) = \sum_{i=1}^m p_i(x) \delta_{z_i}; \quad (4)$$

here, δ_z is the Dirac distribution at the outcome z , and $p = ((p_i(x))_{i=1}^m : x \in \mathcal{X})$ are adjustable probability mass parameters; see Figure 1(a). The number of categories m can be interpreted as controlling the *expressivity* of the representation, and should be carefully chosen in practice.

Dynamic programming. The iteration $\eta \leftarrow \mathcal{T}\eta$ cannot be used to update the parameters p in Equation (4) directly, since the distributions $(\mathcal{T}\eta)(x)$ are no longer supported on $\{z_1, \dots, z_m\}$, and so cannot be expressed in the form given in Equation (4); see Figure 1(c).

Bellemare et al. (2017) circumvent this issue by *projecting* the resulting distributions back onto the support set $\{z_1, \dots, z_m\}$ via a map $\Pi_m : \mathcal{P}([0, (1 - \gamma)^{-1}]) \rightarrow \mathcal{P}(\{z_1, \dots, z_m\})$. Intuitively, Π_m can be thought of as allocating each outcome $z \in [z_i, z_{i+1}]$ to its neighbouring gridpoints z_i and z_{i+1} , in proportion to their proximity, so that the projection of the Dirac distribution δ_z , is defined by

$$\Pi_m \delta_z = \frac{z_{i+1} - z}{z_{i+1} - z_i} \delta_{z_i} + \frac{z - z_i}{z_{i+1} - z_i} \delta_{z_{i+1}}.$$

In this paper, we work with the equivalent definition of the projection Π_m given by Rowland et al. (2018, Proposition 6), in which the probability mass assigned to z_i by $\Pi_m \nu$ is given by the expectation $\mathbb{E}_{Z \sim \nu} [h_i(Z)]$, where $h_i : [0, (1 - \gamma)^{-1}] \rightarrow [0, 1]$ is the ‘‘hat-function’’ at z_i , which linearly interpolates between a value of 1 at z_i , and 0 at neighbouring gridpoints z_{i-1} , z_{i+1} , and is 0 outside this range. Figure 1(b) illustrates h_i and h_m ; see Appendix B for a restatement of the full definition given by Rowland et al. (2018).

Rowland et al. (2018) showed that *categorical dynamic programming* (CDP), the iterative computation $\eta \leftarrow \Pi_m \mathcal{T}\eta$ of *projected* distributional Bellman updates (see Figure 1(c)), leads to convergence of η to a *categorical fixed point*, which can be made arbitrarily close to the true RDF by increasing m , as measured in Cramér distance (Cramér, 1928; Székely, 2003; Székely & Rizzo, 2013).

Definition 2.1. The *Cramér distance* $\ell_2 : \mathcal{P}(\mathbb{R}) \times \mathcal{P}(\mathbb{R}) \rightarrow \mathbb{R}$ is defined by

$$\ell_2(\nu, \nu') = \left[\int_{\mathbb{R}} (F_\nu(t) - F_{\nu'}(t))^2 dt \right]^{1/2},$$

where $F_\nu, F_{\nu'}$ are the CDFs of ν, ν' , respectively. The *supremum-Cramér distance* $\bar{\ell}_2$ on $\mathcal{P}(\mathbb{R})^{\mathcal{X}}$ is defined by

$$\bar{\ell}_2(\eta, \eta') = \max_{x \in \mathcal{X}} \ell_2(\eta(x), \eta'(x)).$$

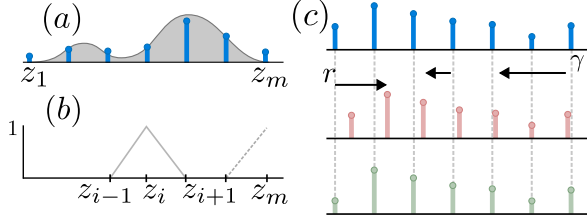


Figure 1. (a) The density of a distribution ν (grey), and its categorical projection $\Pi_m \nu \in \mathcal{P}(\{z_1, \dots, z_m\})$ (blue). (b) Hat functions h_i (solid) and h_m (dashed). (c) A categorical distribution (blue); its update after being scaled by γ and shifted by r by the distributional Bellman operator \mathcal{T} , moving its support off the grid $\{z_1, \dots, z_m\}$ (pink); the resulting realigned distribution supported on the grid $\{z_1, \dots, z_m\}$ after projection via Π_m (green).

The central convergence results concerning CDP established by Rowland et al. (2018) are summarised below.

Proposition 2.2. (Rowland et al., 2018). *The operator $\Pi_m \mathcal{T} : \mathcal{P}([0, (1 - \gamma)^{-1}])^{\mathcal{X}} \rightarrow \mathcal{P}([0, (1 - \gamma)^{-1}])^{\mathcal{X}}$ is a contraction mapping with respect to $\bar{\ell}_2$, with contraction factor $\sqrt{\gamma}$, and has a unique fixed point, $\eta_C \in \mathcal{P}(\{z_1, \dots, z_m\})^{\mathcal{X}}$. As a result, for any $\eta_0 \in \mathcal{P}([0, (1 - \gamma)^{-1}])^{\mathcal{X}}$, with $\eta_{k+1} = \Pi_m \mathcal{T}\eta_k$, we have $\bar{\ell}_2(\eta_k, \eta_C) \leq (1 - \gamma)^{-1} \gamma^k$. Further, the distance between η_C and the true RDF η^* can be bounded as*

$$\bar{\ell}_2(\eta_C, \eta^*) \leq \frac{1}{(1 - \gamma)\sqrt{m - 1}}. \quad (5)$$

This establishes CDP as a principled approach to approximating return distributions, and also quantifies the accuracy achievable with CDP using m categories, which will be central in informing our choice of m to obtain a sample-efficient, accurate algorithm below.

3. Distributional RL with a generative model

The central problem we study in this paper is how to do sample-efficient *distributional* RL with a generative model. That is, given the samples $((X_i^x)_{i=1}^N : x \in \mathcal{X})$ described in Section 2.1, how accurate of an approximation to the return-distribution function in Equation (3) can one compute?

This question was raised by Zhang et al. (2023), who proposed to perform distributional dynamic programming updates $\eta \leftarrow \hat{\mathcal{T}}\eta$ as described in Section 2.2, using the *empirical* distributional Bellman operator $\hat{\mathcal{T}}$ derived from the empirical transition probabilities \hat{P} , producing an estimate $\hat{\eta} \in \mathcal{P}([0, (1 - \gamma)^{-1}])$ of the true RDF η^* such that for any $\varepsilon > 0$ and $\delta \in (0, 1)$,

$$w_1(\hat{\eta}(x), \eta^*(x)) \leq \varepsilon,$$

with probability at least $1 - \delta$ for all $x \in \mathcal{X}$, whenever $N = \tilde{\Omega}(\varepsilon^{-2}(1 - \gamma)^{-4} \text{polylog}(1/\delta))$. Here, w_1 denotes the

Wasserstein-1 distance between probability distributions, defined for any $\nu, \nu' \in \mathcal{P}(\mathbb{R})$ with CDFs $F_\nu, F_{\nu'}$ by

$$w_1(\nu, \nu') = \int_{\mathbb{R}} |F_\nu(t) - F_{\nu'}(t)| dt.$$

We focus on the Wasserstein-1 distance as the main metric of interest in this paper as it is particularly compatible with existing methods for analysing categorical approaches to distributional RL, and it provides upper bounds for differences of many statistical functionals of interest, such as expectations of Lipschitz functions (Villani, 2009; Peyré & Cuturi, 2019); and conditional-value-at-risk (Rockafellar et al., 2000; Rockafellar & Uryasev, 2002; Bhat & Prashanth, 2019, CVaR). Zhang et al. (2023) also prove a lower bound of $N = \tilde{\Omega}(\varepsilon^{-2}(1-\gamma)^{-3})$ samples required to obtain such an accurate prediction with high probability, which follows from a reduction to the mean-return case (Azar et al., 2013), as w_1 -distance upper-bounds difference of means.

There are two natural questions that the analysis of Zhang et al. (2023) leaves open. Firstly, can the gap between the lower bound and upper bound as a function of $(1-\gamma)^{-1}$ described above be closed? Zhang et al. (2023) conjecture that their analysis is loose. Second, we also note that the distributional dynamic programming procedure $\eta \leftarrow \hat{\mathcal{T}}\eta$ proposed by Zhang et al. (2023), without incorporating any restrictions on the representations of distributions, runs into severe space and memory issues, and is not practical to run (and indeed Zhang et al. (2023) introduce approximations to the algorithm when running empirically for these reasons). A remaining question is then whether there are tractable algorithms that can achieve the lower bound on sample complexity described above. Our contributions below provide a new, tractable distributional RL algorithm that attains (up to logarithmic factors) the lower bound on sample complexity provided by Zhang et al. (2023), resolving these questions.

4. Direct categorical fixed-point computation

Our approach to obtaining a sample-efficient algorithm that is near-minimax-optimal in the sense described above begins with the categorical approach to distributional dynamic programming described in Section 2.3. We begin first by introducing a new algorithm for computing the categorical fixed point η_C referred to in Proposition 2.2 *directly*, that avoids computing an approximate solution via dynamic programming iterations $\eta \leftarrow \Pi_m \mathcal{T} \eta$. We expect this algorithm to be of independent interest within distributional reinforcement learning.

4.1. Direct categorical fixed-point computation

Our first contribution is to develop a new computational perspective on the projected categorical Bellman operator $\Pi_m \mathcal{T}$, which results in a new algorithm for computing the

fixed point η_C *exactly*, without requiring the iterative categorical dynamic programming (CDP) algorithm described in Section 2.3.

CDF operator and fixed-point equation. We first formulate the application of the projected categorical Bellman operator $\Pi_m \mathcal{T}$ as a linear map, and give an explicit expression for the matrix representing this linear map when the input RDFs are represented with cumulative distribution functions (CDFs). We consider the effect of applying $\Pi_m \mathcal{T}$ to an RDF $\eta = \mathcal{P}(\{z_1, \dots, z_m\})^{\mathcal{X}}$, with $\eta(x) = \sum_{i=1}^m p_i(x) \delta_{z_i}$. By Rowland et al. (2018, Proposition 6), the updated probabilities for $\Pi_m \mathcal{T}$ can be expressed as

$$p'_i(x) = \sum_{y \in \mathcal{X}} \sum_{j=1}^m P(y|x) h_{i,j}^x p_j(y), \quad (6)$$

where $h_{i,j}^x = h_i(r(x) + \gamma z_j)$. We convert this into an expression for cumulative probabilities, rather than individual probability masses, to obtain a simpler analysis below. To do so, we introduce the encoding of $\eta \in \mathcal{P}(\{z_1, \dots, z_m\})^{\mathcal{X}}$ into corresponding CDF values $F \in \mathbb{R}^{\mathcal{X} \times m}$, where $F_i(x) = \eta(x)([z_1, z_i])$ denotes the *cumulative* mass for the distribution at state x over the set $\{z_1, \dots, z_i\}$.

Proposition 4.1. *If $\eta \in \mathcal{P}(\{z_1, \dots, z_m\})^{\mathcal{X}}$ is an RDF with corresponding CDF values $F \in \mathbb{R}^{\mathcal{X} \times m}$, then the corresponding CDF values $F' \in \mathbb{R}^{\mathcal{X} \times m}$ for $\Pi_m \mathcal{T} \eta$ satisfy*

$$F'_i(x) = \sum_{y \in \mathcal{X}} \sum_{j=1}^m P(y|x) (H_{i,j}^x - H_{i,j+1}^x) F_j(y), \quad (7)$$

where

$$H_{i,j}^x = \sum_{l \leq i} h_l(r(x) + \gamma z_j) \quad (8)$$

for $j = 1, \dots, m$, and by convention we take $H_{i,m+1}^x = 0$.

Under this notation, we can rewrite Equation (7) simply as a matrix-vector multiplication in the space $\mathbb{R}^{\mathcal{X} \times [m]}$:

$$F' = T_P F,$$

where T_P is the $(\mathcal{X} \times [m]) \times (\mathcal{X} \times [m])$ square matrix, with entries given by

$$T_P(x, i; y, j) = P(y|x) (H_{i,j}^x - H_{i,j+1}^x), \quad (9)$$

and $F, F' \in \mathbb{R}^{\mathcal{X} \times m}$ above are interpreted in vectorised form. We drop dependence on m from the notation T_P for conciseness. Thus, CDP can be implemented via simple matrix multiplication on CDF values, and the CDF values F^* corresponding to the categorical fixed point η_C solve the equation

$$F = T_P F, \text{ or equivalently } (I - T_P)F = 0. \quad (10)$$

Obtaining a system with unique solution. Equation (10) suggests that we can directly solve a linear system to obtain the exact categorical fixed point, rather than performing the iterative CDP algorithm to obtain an approximation. Note, however, that F^* is not the *unique* solution of Equation (10); for example, $F = 0$ is also a solution. This arises because in Equation (10), the *distribution masses* at each state (that is, $F_m(x)$), are unconstrained. By contrast, Proposition 2.2 establishes that η_C is the unique solution of $\eta = \Pi_m \mathcal{T} \eta$ in the space $\mathcal{P}([z_1, z_m])^{\mathcal{X}}$, where each element $\eta(x)$ is constrained to be a probability distribution *a priori*. Thus, Equation (10) requires some modification to obtain a linear system with a unique solution. This is obtained by removing $F_m(x)$ as a variable from the system (for each $x \in \mathcal{X}$), replacing it by the constant 1, and removing redundant rows from the resulting linear system, as the following proposition describes; the “axis-aligned” nature of these constraints is the benefit of working with CDF values.

Proposition 4.2. *The linear system in Equation (10), with the additional linear constraints $F_m(x) = 1$ for all $x \in \mathcal{X}$, is equivalent to the following linear system in $\tilde{F} \in \mathbb{R}^{\mathcal{X} \times [m-1]}$:*

$$(I - \tilde{T}_P)\tilde{F} = \tilde{H}, \quad (11)$$

where the $(x, i; y, j)$ coordinate of \tilde{T}_P (for $1 \leq i, j \leq m-1$) is

$$\tilde{T}_P(x, i; y, j) = P(y|x)(H_{i,j}^x - H_{i,j+1}^x),$$

and for each $x \in \mathcal{X}$, $1 \leq i \leq m-1$:

$$\tilde{H}(x, i) = H_{i,m}^x.$$

Having moved to the inhomogeneous system over $\mathbb{R}^{\mathcal{X} \times [m-1]}$ in Equation (11), we can deduce the following via the contraction theory in Proposition 2.2.

Proposition 4.3. *The linear system in Equation (11) has a unique solution, which is precisely the CDF values $((F_i^*(x))_{i=1}^{m-1} : x \in \mathcal{X})$ of the categorical fixed point.*

The *direct categorical fixed-point algorithm* (DCFP) consists of solving the linear system in Equation (11) to obtain the exact categorical fixed point; see Algorithm 1 for a summary.

Algorithm 1 DCFP

- 1: Calculate matrices $(H^x : x \in \mathcal{X})$ via Equation (8).
 - 2: Calculate matrix \tilde{T}_P and vector \tilde{H} via Equation (9).
 - 3: Call linear system solver on Equation (11).
 - 4: Obtain resulting solution $\tilde{F}^* \in \mathbb{R}^{\mathcal{X} \times [m-1]}$.
 - 5: Return F^* , obtained by appending the values $F_m^*(x) = 1$ to the solution \tilde{F}^* .
-

Complexity and implementation details. Representing \tilde{T}_P as a dense matrix requires $O(|\mathcal{X}|^2 m^2)$ space, and solving the corresponding linear system in Equation (11) with a standard linear solver requires $O(|\mathcal{X}|^3 m^3)$ time. However, in many problems there are cases where the DCFP algorithm can be implemented more efficiently. Crucially, \tilde{T}_P often has sparse structure, and so sparse linear solvers may afford an opportunity to make substantial improvements in computational efficiency. We explore this point further empirically in Section 6, and discuss the sparsity the linear system from a theoretical perspective in Appendix F.

4.2. DCFP with a generative model

We now return to the setting where the Markov reward process in which we are performing evaluation is unknown, and instead we have access to the random next-state samples $((X_i^x)_{i=1}^N : x \in \mathcal{X})$, as described in Section 3.

Our model-based DCFP algorithm proceeds by first constructing the corresponding empirical transition probabilities \hat{P} , so that $\hat{P}(y|x) = N^{-1} \sum_{i=1}^N \mathbb{1}\{X_i^x = y\}$, and then calls the DCFP procedure outlined in Algorithm 1, treating \hat{P} as the true transition probabilities of the MRP when constructing the matrix in Line 1, which we denote here by $T_{\hat{P}}$, to reflect the fact that it is built from \hat{P} . This produces the output CDF values \hat{F} , from which estimated return distributions can be decoded as

$$\hat{\eta}(x) = \sum_{i=1}^m (\hat{F}_i(x) - \hat{F}_{i-1}(x)) \delta_{z_i}, \quad (12)$$

where by convention $F_0(x) = 0$.

5. Sample complexity analysis

Our goal now is to analyse the sample complexity of model-based DCFP, as described in the previous section. We first introduce a notational shorthand that will be of extensive use in the statement and proof of this result: when writing distances between distributions, such as $w_1(\eta^*(x), \hat{F}(x))$, we identify CDF vectors $\hat{F}(x) \in \mathbb{R}^m$ with the distributions they represent as in Equation (12). The core theoretical result of the paper is as follows.

Theorem 5.1. *Let $\varepsilon \in (0, (1 - \gamma)^{-1/2})$ and $\delta \in (0, 1)$, and suppose the number of categories satisfies $m \geq 4(1 - \gamma)^{-2} \varepsilon^{-2} + 1$. Then the output \hat{F} of model-based DCFP with $N = \Omega(\varepsilon^{-2} (1 - \gamma)^{-3} \text{polylog}(|\mathcal{X}|/\delta))$ samples satisfies*

$$\max_{x \in \mathcal{X}} w_1(\eta^*(x), \hat{F}(x)) \leq \varepsilon,$$

with probability at least $1 - \delta$.

This result establishes that model-based DCFP attains the minimax lower-bound (up to logarithmic factors) for high-probability return distribution estimation in Wasserstein

distance, resolving an open question raised by Zhang et al. (2023); in a certain sense, *estimation of return distributions is no more statistically difficult than that of mean returns with a generative model*. We emphasise that there is no direct dependence of N on m , so there is no statistical penalty to using a large number of categories m .

5.1. Structure of the proof of Theorem 5.1

The remainder of this section provides a sketch proof of Theorem 5.1; a complete proof is provided in the appendix. The proof is broadly motivated by the approaches of Azar et al. (2013), Agarwal et al. (2020), and Pananjady & Wainwright (2020), who analyse the mean-return case, and we highlight where key ideas and new mathematical objects are required in this distributional setting. In particular, we highlight the use of the *stochastic categorical CDF Bellman equation*, a new distributional Bellman equation that plays a key role in our analysis, which we expect to be of independent interest.

Reduction to Cramér distance. The first step of the analysis is to reduce Theorem 5.1 to a statement about approximation in Cramér distance, which is much better suited to the analysis of DCFP, owing to the results described in Section 2.3. This can be done by upper-bounding Wasserstein distance by Cramér distance using the following result, which is proven in the appendix via Jensen’s inequality.

Lemma 5.2. *For any two distributions $\nu, \nu' \in \mathcal{P}([0, (1 - \gamma)^{-1}])$, we have*

$$w_1(\nu, \nu') \leq (1 - \gamma)^{-1/2} \ell_2(\nu, \nu').$$

Theorem 5.1 now follows from the following result, which quantifies the sample complexity of model-based DCFP when measuring distances using the Cramér distance.

Theorem 5.3. *Let $\varepsilon \in (0, 1)$ and $\delta \in (0, 1)$, and suppose the number of categories satisfies $m \geq 4(1 - \gamma)^{-2}\varepsilon^{-2} + 1$. Then the output \hat{F} of model-based DCFP with $N = \Omega(\varepsilon^{-2}(1 - \gamma)^{-2}\text{polylog}(|\mathcal{X}|/\delta))$ samples satisfies*

$$\max_{x \in \mathcal{X}} \ell_2(\eta^*(x), \hat{F}(x)) \leq \varepsilon, \quad (13)$$

with probability at least $1 - \delta$.

Reduction to categorical fixed-point error. Our first step in proving Theorem 5.3 is to use the triangle inequality to split the Cramér distance on the left-hand side of Equation (13) into a representation approximation error, and sample-based error:

$$\begin{aligned} \bar{\ell}_2(\eta^*, \hat{F}) &\leq \bar{\ell}_2(\eta^*, F^*) + \bar{\ell}_2(F^*, \hat{F}) \\ &\leq \frac{1}{(1 - \gamma)\sqrt{m - 1}} + \bar{\ell}_2(F^*, \hat{F}), \end{aligned}$$

with the second inequality following from the fixed-point quality bound in Equation (5). With m as specified in the

theorem statement, the first term in the right-hand side above is bounded by $\varepsilon/2$. Thus, it suffices to focus on the second term on the right-hand side, which quantifies the sample-based error in estimating the categorical fixed point F^* .

Concentration. Through a combination of the use of a version of Bernstein’s inequality in Hilbert space (Chatalic et al., 2022) and propagation of this inequality across time steps in the MRP, we next arrive at the following inequality with probability at least $1 - \delta$:

$$\begin{aligned} \ell_2(\hat{F}(x), F^*(x)) &\leq \\ &\tilde{O}\left(\frac{1}{\sqrt{N(1 - \gamma)}} \sqrt{\|(I - \gamma\hat{P})^{-1}\sigma_{\hat{P}}\|_\infty} + \frac{1}{(1 - \gamma)^{3/2}N^{3/4}}\right). \end{aligned} \quad (14)$$

Here, $\sigma_{\hat{P}} \in \mathbb{R}^{\mathcal{X}}$ is an instance of a new class of distributional object, the *local squared-Cramér variation*. The general definition of this object is given below, for the case of a general transition matrix $Q \in \mathbb{R}^{\mathcal{X} \times \mathcal{X}}$, to avoid conflation with the specific transition matrices P and \hat{P} that Theorem 5.3 is concerned with.

Definition 5.4. For a given transition matrix Q , the *single-sample operator* $\hat{T}_Q : \mathbb{R}^{\mathcal{X} \times m} \rightarrow \mathbb{R}^{\mathcal{X} \times m}$ is the random operator given by: (i) constructing a *random transition matrix* \hat{Q} by, for each $x \in \mathcal{X}$, sampling $X' \sim Q(\cdot|x)$, and setting $\hat{Q}(X'|x) = 1$; (ii) setting $\hat{T}_Q = T_{\hat{Q}}$.

Definition 5.5. For a given transition matrix Q with corresponding CDP fixed point $F^Q \in \mathbb{R}^{\mathcal{X} \times m}$, the *local squared-Cramér variation at Q* , $\sigma_Q \in \mathbb{R}^{\mathcal{X}}$, is defined by

$$\sigma_Q(x) = \mathbb{E}[\ell_2^2((\hat{T}_Q F^Q)(x), F^Q(x))].$$

Intuitively, the local squared-Cramér variation σ_Q encodes the variability of the fixed point F^Q after a sample-based, rather than exact, dynamic programming update. From this point of view, it is a natural quantity to arise in Equation (14), and plays a similar role to the variance in the classical Bernstein inequality (Bernstein, 1946).

In Corollary 5.12 below, we will deduce that under the conditions of Theorem 5.3, we have

$$\|(I - \gamma\hat{P})^{-1}\sigma_{\hat{P}}\|_\infty \leq \frac{2}{1 - \gamma}. \quad (15)$$

Substituting this into Equation (14) gives

$$\ell_2(\hat{F}(x), F^*(x)) \leq \tilde{O}\left(\frac{1}{(1 - \gamma)\sqrt{N}} + \frac{1}{(1 - \gamma)^{3/2}N^{3/4}}\right)$$

with probability at least $1 - \delta$, for all $x \in \mathcal{X}$. Now, taking $N = \tilde{\Omega}((1 - \gamma)^{-2}\varepsilon^{-2})$ yields that this expression is $O(\varepsilon)$, which completes the sketch proof of Theorem 5.3.

What remains to be described is how to arrive at the bound in Equation (15); The section below provides a high-level overview of the technical details involved in obtaining it.

5.2. The stochastic categorical CDF Bellman equation

The central idea is to relate the *local* squared-Cramér variation to a corresponding *global* notion of variation, in analogy with the variance Bellman equation (Sobel, 1982) used by Azar et al. (2013) in the mean-return case. To define this corresponding global notion, we begin by defining a new type of distributional Bellman equation, which can be intuitively thought of as encoding the result of repeatedly applying a sequence of independent single-sample operators. Again, we work with a general transition matrix Q .

Definition 5.6. For a general transition matrix Q , the *stochastic categorical CDF (SC-CDF) Bellman equation* is given by

$$\Phi(x) \stackrel{\mathcal{D}}{=} (\hat{T}_Q \Phi)(x), \quad (16)$$

where $\stackrel{\mathcal{D}}{=}$ denotes equality in distribution. Here, \hat{T}_Q is a *single-sample operator* with respect to Q , as in Definition 5.4. Each $\Phi(x)$ is a random variable taking values in the space of valid CDF values

$$\mathcal{F} = \{F \in \mathbb{R}^m : 0 \leq F_1 \leq \dots \leq F_{m-1} \leq F_m = 1\}$$

for distributions in $\mathcal{P}(\{z_1, \dots, z_m\})$, and importantly is taken to be independent of the random operator \hat{T}_Q .

The intuition is that “unravelling” Equation (16) should lead to a solution of the form $\Phi(x) \stackrel{\mathcal{D}}{=} \lim_{k \rightarrow \infty} \hat{T}_Q^{(k)} \dots \hat{T}_Q^{(1)} F$, where $(\hat{T}_Q^{(i)})_{i=1}^k$ are independent single-sample operators, so that $\Phi(x)$ encodes the fluctuations due to repeated CDP updates with randomly-sampled transitions. To make this intuition precise, we first verify that the SC-CDF Bellman equation has a unique solution.

Proposition 5.7. *The SC-CDF Bellman equation in Equation (16) has a unique solution, in the sense that there is a unique distribution for each $\Phi(x)$ such that Equation (16) holds for each $x \in \mathcal{X}$.*

We write Φ^Q for the collection of random CDFs that satisfy the SC-CDF Bellman equation in Equation (16), whose existence is guaranteed by Proposition 5.7. We next relate Φ^Q to the standard categorical fixed point F^Q .

Proposition 5.8. *We have $\mathbb{E}[\Phi^Q(x)] = F^Q(x)$ for all $x \in \mathcal{X}$.*

Proposition 5.8 shows that Φ^Q can indeed be thought of as encoding random variation around the usual categorical fixed point F^Q ; see Figure 2. This motivates the following.

Definition 5.9. For a given transition matrix Q with corresponding CDP fixed point $F^Q \in \mathbb{R}^{\mathcal{X} \times m}$, the *global squared-Cramér variation at Q* , $\Sigma_Q \in \mathbb{R}^{\mathcal{X}}$, is defined by

$$\Sigma_Q(x) = \mathbb{E}[\ell_2^2(\Phi^Q(x), F^Q(x))].$$

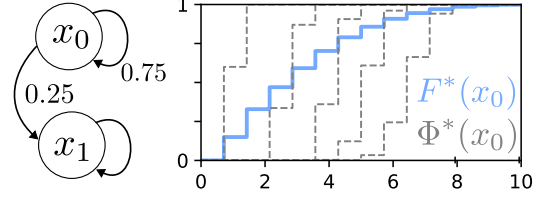


Figure 2. Left: Example MRP with $r(x_0) = 1, r(x_1) = 0, \gamma = 0.9$. Right: Categorical fixed point $F^*(x_0)$ with $m = 15$, and 5 independent samples from the random CDF $\Phi^*(x_0)$.

Remark 5.10. *We pause to consider the nature of the new object defined by the SC-CDF Bellman equation; $\Phi^Q(x)$ is a doubly distributional object. It represents a probability distribution around the object $F^Q(x)$, which itself already summarises the distribution of the return. This reveals a dual perspective on distributional RL itself: the randomness modelled can be: (i) of intrinsic interest, and/or (ii) instrumental in analysing the estimation of a non-random object from random data (c.f. the variance Bellman equation in analysing the estimation of mean returns (Azar et al., 2013)). The object Φ^Q is motivated by both of these concerns.*

The following Bellman-like inequality draws a relationship between local and global squared-Cramér variation, allowing us to make progress from Equation (15).

Proposition 5.11. *We have*

$$\Sigma_Q \geq \sigma_Q + \gamma Q \Sigma_Q - \left(\frac{2}{m\sqrt{1-\gamma}} + \frac{1}{m^2(1-\gamma)^2} \right) \mathbf{1},$$

where $\mathbf{1} \in \mathbb{R}^{\mathcal{X}}$ is a vector of ones, and the inequality above is interpreted component-wise.

Rearrangement and bounding of the quantities in the inequality of Proposition 5.11, in the specific case $Q = \hat{P}$, then allows us to deduce the required inequality in Equation (15) that completes the proof of Theorem 5.3.

Corollary 5.12. *We can bound the term $\|(I - \gamma \hat{P})^{-1} \sigma_{\hat{P}}\|_\infty$ appearing in Equation (14) under the assumptions of Theorem 5.3 as follows:*

$$\|(I - \gamma \hat{P})^{-1} \sigma_{\hat{P}}\|_\infty \leq \|\Sigma_{\hat{P}}\|_\infty + \frac{1}{1-\gamma} \leq \frac{2}{1-\gamma}.$$

6. Empirical evaluation

To complement our theoretical analysis, which focuses on worst-case sample complexity bounds, we report empirical findings for implementations of several model-based distributional RL algorithms in the generative model setting. We compare the new DCFP algorithm introduced in Section 4.1 with *quantile dynamic programming* (Dabney et al., 2018b; Bellemare et al., 2023, QDP) a distinct approach to distributional RL in which return distributions are approximated via dynamic programming with a finite number of quantiles.

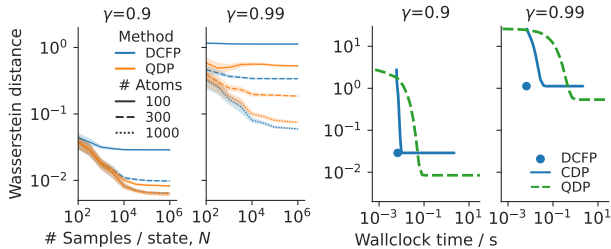


Figure 3. Wasserstein-1 approximation error and wallclock time for a variety of distributional RL methods, discount factors, numbers of atoms, and numbers of environment samples.

In Figure 3 (left), we report results of running DCFP and QDP on a 5-state environment with transition matrix randomly sampled from Dirichlet distributions, and entries of the immediate reward function $r \in \mathbb{R}^{\mathcal{X}}$ randomly sampled from $\text{Unif}([0, 1])$, with varying numbers of atoms m , environment samples per state N , and discount γ . We report the maximum w_1 -error against true return distributions (estimated via Monte Carlo sampling). All runs are repeated 30 times, and error bars are 95% bootstrapped confidence intervals. Sufficient DP iterations ensure approximate convergence to their fixed points. In Figure 3 (right), we plot estimation error against wallclock time for $m = 100$, $N = 10^6$, including results for CDP (which approximates the solution of DCFP via dynamic programming; Section 2.3); line plots indicate the estimation error/wallclock time trade-off as we increase the number of DP iterations.

For low discount factors/atom counts QDP generally outperforms DCFP in terms of asymptotic estimation error, due to QDP’s ability to modify its atom support to regions of the interval $[0, (1-\gamma)^{-1}]$ where mass is concentrated. However, we note that DCFP is generally faster than QDP. Further, the gap between DCFP and QDP, in terms of estimation error, is vastly reduced for larger discount and larger atom count. We also note that particularly at high discounts, DCFP outperforms CDP and QDP in terms of wallclock time, due to DP methods requiring many iterations to converge in these cases (Rowland et al., 2018; Dabney et al., 2018b). Full results, including on several further environments, are given in Appendix F: key findings include that QDP works particularly well in near-deterministic environments, and DCFP works particularly well in settings where there are short high-probability paths from a state to itself. We also investigate versions of DCFP and CDP that set atom locations $(z_i)_{i=1}^m$ based on environment-specific information, which can significantly perform the accuracy of these methods for a given atom count m .

7. Related work and directions for future work

Here, we describe the most salient aspects of related work, and promising directions for future work; an extended dis-

ussion is given in Appendix A.

Alternative distributional RL algorithms. Our analysis has focused on categorical distributional RL, and in particular has made use of linearity of the corresponding CDF DP operator both as a function of input CDFs, and of transition probabilities. Our experiments also compare against QDP, a tabular dynamic programming version of a widely used approach to distributional RL based on quantiles; these results suggest strong theoretical bounds may also be possible for QDP, although the non-linearity of the operator may complicate the analysis. Investigation of other approaches such as fitted likelihood evaluation (Wu et al., 2023, FLE), in the generative model setting, is another interesting direction.

Other statistical questions in distributional RL. Zhang et al. (2023) make several other contributions on the topic of statistical estimation in distributional RL, including analysis of asymptotic fluctuations and limit theorems. Wu et al. (2023) study the offline evaluation problem, in which state-action pairs are sampled from the stationary distribution of the policy, via FLE and focus on generalisation bounds. Böck & Heirzinger (2022) propose a *model-free* algorithm for distributional RL, *speedy categorical TD-learning*, motivated by categorical TD learning (Rowland et al., 2018) and speedy Q-learning (Azar et al., 2011), and prove a sample complexity bound of $\tilde{O}(\varepsilon^{-2}(1-\gamma)^{-3})$ for high probability ε -accurate estimation in Cramér distance, implying a sample complexity of $\tilde{O}(\varepsilon^{-2}(1-\gamma)^{-4})$ in w_1 , by Lemma 5.2.

Risk-sensitive control. The theory developed in this paper has focused on estimation of return distributions for individual policies. A natural direction for future work is to analyse identification of near-optimal policies for risk-sensitive decision criteria. Bastani et al. (2022); Wang et al. (2023a) study efficient algorithms for CVaR optimisation, while Fei et al. (2021a;b); Liang & Luo (2022) study entropic risk maximisation, and Du et al. (2022); Lam et al. (2022) study iterated CVaR optimisation, all in the *online* setting.

8. Conclusion

We have introduced a new algorithm, DCFP, for directly computing the fixed point of CDP, a widely used distributional reinforcement learning algorithm. We then showed that this algorithm, with an appropriately chosen number of categories m , achieves the minimax lower bound (up to logarithmic factors) for sample complexity of return-distribution estimation in Wasserstein distance obtained by Zhang et al. (2023). Thus, this paper closes an open question raised by Zhang et al. (2023) by exhibiting an algorithm that obtains this lower bound, and shows that estimation of return distributions via a generative model is no harder statistically than the analogous task for mean returns. Our analysis also requires the introduction of the novel stochastic categorical

CDF Bellman equation, which we expect to be of independent interest, and our empirical study reveals several important take-aways for practitioners, including findings that the optimal choice distributional RL algorithm may depend on several particular aspects of the environment.

Acknowledgements

We thank Dave Abel for detailed comments on a draft version of the paper. We also thank Mohammad Gheshlaghi Azar for useful conversations, and Arthur Gretton for advice on Bernstein-like inequalities in Hilbert space.

References

- Agarwal, A., Kakade, S., and Yang, L. F. Model-based reinforcement learning with a generative model is minimax optimal. In *Conference on Learning Theory*, 2020.
- Azar, M. G., Munos, R., Ghavamzadeh, M., and Kappen, H. Speedy Q-learning. In *Advances in Neural Information Processing Systems*, 2011.
- Azar, M. G., Munos, R., and Kappen, H. J. Minimax PAC bounds on the sample complexity of reinforcement learning with a generative model. *Machine learning*, 91:325–349, 2013.
- Bastani, O., Ma, J. Y., Shen, E., and Xu, W. Regret bounds for risk-sensitive reinforcement learning. In *Advances in Neural Information Processing Systems*, 2022.
- Bellemare, M. G., Dabney, W., and Munos, R. A distributional perspective on reinforcement learning. In *Proceedings of the International Conference on Machine Learning*, 2017.
- Bellemare, M. G., Candido, S., Castro, P. S., Gong, J., Machado, M. C., Moitra, S., Ponda, S. S., and Wang, Z. Autonomous navigation of stratospheric balloons using reinforcement learning. *Nature*, 588(7836):77–82, 2020.
- Bellemare, M. G., Dabney, W., and Rowland, M. *Distributional Reinforcement Learning*. MIT Press, 2023. <http://www.distributional-rl.org>.
- Bernstein, S. *The Theory of Probabilities*. Gastehizdat Publishing House, 1946.
- Bhat, S. P. and Prashanth, L. A. Concentration of risk measures: A Wasserstein distance approach. In *Advances in Neural Information Processing Systems*, 2019.
- Böck, M. and Heitzinger, C. Speedy categorical distributional reinforcement learning and complexity analysis. *SIAM Journal on Mathematics of Data Science*, 4(2): 675–693, 2022.
- Böck, M., Malle, J., Pasterk, D., Kukina, H., Hasani, R., and Heitzinger, C. Superhuman performance on sepsis MIMIC-III data by distributional reinforcement learning. *PLoS One*, 17(11):e0275358, 2022.
- Bodnar, C., Li, A., Hausman, K., Pastor, P., and Kalakrishnan, M. Quantile QT-Opt for risk-aware vision-based robotic grasping. In *Robotics: Science and Systems*, 2020.
- Chandak, Y., Shankar, S., and Thomas, P. S. High-confidence off-policy (or counterfactual) variance estimation. In *Proceedings of the AAAI Conference on Artificial Intelligence*, 2021.
- Chatalic, A., Schreuder, N., Rosasco, L., and Rudi, A. Nyström kernel mean embeddings. In *Proceedings of the International Conference on Machine Learning*, 2022.
- Cramér, H. On the composition of elementary errors. *Scandinavian Actuarial Journal*, 1928(1):13–74, 1928.
- Dabney, W., Ostrovski, G., Silver, D., and Munos, R. Implicit quantile networks for distributional reinforcement learning. In *Proceedings of the International Conference on Machine Learning*, 2018a.
- Dabney, W., Rowland, M., Bellemare, M. G., and Munos, R. Distributional reinforcement learning with quantile regression. In *Proceedings of the AAAI Conference on Artificial Intelligence*, 2018b.
- Dabney, W., Kurth-Nelson, Z., Uchida, N., Starkweather, C. K., Hassabis, D., Munos, R., and Botvinick, M. A distributional code for value in dopamine-based reinforcement learning. *Nature*, 577(7792):671–675, 2020.
- Doan, T., Mazouze, B., and Lyle, C. GAN Q-learning. *arXiv*, 2018.
- Du, Y., Wang, S., and Huang, L. Provably efficient risk-sensitive reinforcement learning: Iterated CVaR and worst path. In *Proceedings of the International Conference on Learning Representations*, 2022.
- Dvoretzky, A., Kiefer, J., and Wolfowitz, J. Asymptotic minimax character of the sample distribution function and of the classical multinomial estimator. *The Annals of Mathematical Statistics*, pp. 642–669, 1956.
- Fawzi, A., Balog, M., Huang, A., Hubert, T., Romera-Paredes, B., Barekatin, M., Novikov, A., R Ruiz, F. J., Schrittwieser, J., Swirszcz, G., Silver, D., Hassabis, D., and Kohli, P. Discovering faster matrix multiplication algorithms with reinforcement learning. *Nature*, 610(7930): 47–53, 2022.
- Fei, Y., Yang, Z., Chen, Y., and Wang, Z. Exponential bellman equation and improved regret bounds for risk-sensitive reinforcement learning. In *Advances in Neural Information Processing Systems*, 2021a.

- Fei, Y., Yang, Z., and Wang, Z. Risk-sensitive reinforcement learning with function approximation: A debiasing approach. In *Proceedings of the International Conference on Machine Learning*, 2021b.
- Freirich, D., Shimkin, T., Meir, R., and Tamar, A. Distributional multivariate policy evaluation and exploration with the Bellman GAN. In *Proceedings of the International Conference on Machine Learning*, 2019.
- Gretton, A., Borgwardt, K. M., Rasch, M. J., Schölkopf, B., and Smola, A. A kernel two-sample test. *The Journal of Machine Learning Research*, 13(1):723–773, 2012.
- Harris, C. R., Millman, K. J., van der Walt, S. J., Gommers, R., Virtanen, P., Cournapeau, D., Wieser, E., Taylor, J., Berg, S., Smith, N. J., Kern, R., Picus, M., Hoyer, S., van Kerkwijk, M. H., Brett, M., Haldane, A., del Río, J. F., Wiebe, M., Peterson, P., Gérard-Marchant, P., Sheppard, K., Reddy, T., Weckesser, W., Abbasi, H., Gohlke, C., and Oliphant, T. E. Array programming with NumPy. *Nature*, 585(7825):357–362, September 2020. doi: 10.1038/s41586-020-2649-2.
- Hunter, J. D. Matplotlib: A 2d graphics environment. *Computing in Science & Engineering*, 9(3):90–95, 2007.
- Kakade, S. M. *On the sample complexity of reinforcement learning*. PhD thesis, University College London, 2003.
- Kearns, M., Mansour, Y., and Ng, A. Y. A sparse sampling algorithm for near-optimal planning in large Markov decision processes. *Machine learning*, 49:193–208, 2002.
- Lam, T., Verma, A., Low, B. K. H., and Jaillet, P. Risk-aware reinforcement learning with coherent risk measures and non-linear function approximation. In *Proceedings of the International Conference on Learning Representations*, 2022.
- Li, G., Wei, Y., Chi, Y., Gu, Y., and Chen, Y. Breaking the sample size barrier in model-based reinforcement learning with a generative model. In *Advances in Neural Information Processing Systems*, 2020.
- Liang, H. and Luo, Z.-Q. Bridging distributional and risk-sensitive reinforcement learning with provable regret bounds. *arXiv*, 2022.
- Massart, P. The tight constant in the Dvoretzky-Kiefer-Wolfowitz inequality. *The Annals of Probability*, pp. 1269–1283, 1990.
- Morimura, T., Sugiyama, M., Kashima, H., Hachiya, H., and Tanaka, T. Nonparametric return distribution approximation for reinforcement learning. In *Proceedings of the International Conference on Machine Learning*, 2010a.
- Morimura, T., Sugiyama, M., Kashima, H., Hachiya, H., and Tanaka, T. Parametric return density estimation for reinforcement learning. In *Proceedings of the Conference on Uncertainty in Artificial Intelligence*, 2010b.
- Nguyen-Tang, T., Gupta, S., and Venkatesh, S. Distributional reinforcement learning via moment matching. In *Proceedings of the AAAI Conference on Artificial Intelligence*, 2021.
- Pananjady, A. and Wainwright, M. J. Instance-dependent ℓ_∞ -bounds for policy evaluation in tabular reinforcement learning. *IEEE Transactions on Information Theory*, 67(1):566–585, 2020.
- Peyré, G. and Cuturi, M. *Computational optimal transport: With applications to data science*. Foundations and Trends® in Machine Learning. Now Publishers, Inc., 2019.
- Puterman, M. L. *Markov decision processes: Discrete stochastic dynamic programming*. John Wiley & Sons, 2014.
- Rockafellar, R. T. and Uryasev, S. Conditional value-at-risk for general loss distributions. *Journal of banking & finance*, 26(7):1443–1471, 2002.
- Rockafellar, R. T., Uryasev, S., et al. Optimization of conditional value-at-risk. *Journal of risk*, 2:21–42, 2000.
- Rowland, M., Bellemare, M. G., Dabney, W., Munos, R., and Teh, Y. W. An analysis of categorical distributional reinforcement learning. In *Proceedings of the International Conference on Artificial Intelligence and Statistics*, 2018.
- Rowland, M., Munos, R., Azar, M. G., Tang, Y., Ostrovski, G., Harutyunyan, A., Tuyls, K., Bellemare, M. G., and Dabney, W. An analysis of quantile temporal-difference learning. *arXiv*, 2023.
- Sejdinovic, D., Sriperumbudur, B., Gretton, A., and Fukumizu, K. Equivalence of distance-based and RKHS-based statistics in hypothesis testing. *The Annals of Statistics*, pp. 2263–2291, 2013.
- Shahriari, B., Abdolmaleki, A., Byravan, A., Friesen, A., Liu, S., Springenberg, J. T., Heess, N., Hoffman, M., and Riedmiller, M. Revisiting gaussian mixture critics in off-policy reinforcement learning: A sample-based approach. *arXiv*, 2022.
- Sidford, A., Wang, M., Wu, X., Yang, L., and Ye, Y. Near-optimal time and sample complexities for solving Markov decision processes with a generative model. *Advances in Neural Information Processing Systems*, 2018.

- Sobel, M. J. The variance of discounted Markov decision processes. *Journal of Applied Probability*, 19(4):794–802, 1982.
- Székely, G. J. E-statistics: The energy of statistical samples. Technical Report 05, Bowling Green State University, Department of Mathematics and Statistics Technical Report, 2003.
- Székely, G. J. and Rizzo, M. L. Energy statistics: A class of statistics based on distances. *Journal of statistical planning and inference*, 143(8):1249–1272, 2013.
- Van Rossum, G. and Drake, F. L. *Python 3 Reference Manual*. CreateSpace, Scotts Valley, CA, 2009.
- Villani, C. *Optimal transport: Old and new*, volume 338. Springer, 2009.
- Virtanen, P., Gommers, R., Oliphant, T. E., Haberland, M., Reddy, T., Cournapeau, D., Burovski, E., Peterson, P., Weckesser, W., Bright, J., van der Walt, S. J., Brett, M., Wilson, J., Millman, K. J., Mayorov, N., Nelson, A. R. J., Jones, E., Kern, R., Larson, E., Carey, C. J., Polat, İ., Feng, Y., Moore, E. W., VanderPlas, J., Laxalde, D., Perktold, J., Cimrman, R., Henriksen, I., Quintero, E. A., Harris, C. R., Archibald, A. M., Ribeiro, A. H., Pedregosa, F., van Mulbregt, P., and SciPy 1.0 Contributors. SciPy 1.0: Fundamental Algorithms for Scientific Computing in Python. *Nature Methods*, 17:261–272, 2020.
- Wang, K., Kallus, N., and Sun, W. Near-minimax-optimal risk-sensitive reinforcement learning with CVaR. In *Proceedings of the International Conference on Machine Learning*, 2023a.
- Wang, K., Zhou, K., Wu, R., Kallus, N., and Sun, W. The benefits of being distributional: Small-loss bounds for reinforcement learning. *arXiv*, 2023b.
- Wang, Z., Gao, Y., Wang, S., Zavlanos, M. M., Abate, A., and Johansson, K. H. Policy evaluation in distributional LQR (extended version). *arXiv*, 2023c.
- Waskom, M. L. seaborn: statistical data visualization. *Journal of Open Source Software*, 6(60):3021, 2021.
- Wu, R., Uehara, M., and Sun, W. Distributional offline policy evaluation with predictive error guarantees. In *Proceedings of the International Conference on Machine Learning*, 2023.
- Wurman, P. R., Barrett, S., Kawamoto, K., MacGlashan, J., Subramanian, K., Walsh, T. J., Capobianco, R., Devlic, A., Eckert, F., Fuchs, F., Gilpin, L., Khandelwal, P., Kompella, V., Lin, H., MacAlpine, P., Oller, D., Seno, T., Sherstan, C., Thomure, M. D., Aghabozorgi, H., Barrett, L., Douglas, R., Whitehead, D., Dürr, P., Stone, P., Spranger, M., and Kitano, H. Outracing champion Gran Turismo drivers with deep reinforcement learning. *Nature*, 602(7896):223–228, 2022.
- Yang, D., Zhao, L., Lin, Z., Qin, T., Bian, J., and Liu, T.-Y. Fully parameterized quantile function for distributional reinforcement learning. In *Advances in Neural Information Processing Systems*, 2019.
- Yue, Y., Wang, Z., and Zhou, M. Implicit distributional reinforcement learning. In *Advances in Neural Information Processing Systems*, 2020.
- Yurinsky, V. *Sums and Gaussian vectors*. Springer, 2006.
- Zhang, L., Peng, Y., Liang, J., Yang, W., and Zhang, Z. Estimation and inference in distributional reinforcement learning. *arXiv*, 2023.

APPENDICES:

Near-Minimax-Optimal Distributional Reinforcement Learning with a Generative Model

For convenience, we provide a summary of the contents of the appendices below.

- Appendix A expands on the discussion of related work given in Section 7 in the main paper.
- Appendix B provides additional convenient notation for the categorical CDF operator $T_{\mathcal{P}}$, in particular expressing it as the combination of a scaling/shifting/projecting operation, and a mixing operation over the state to be bootstrapped from. Several additional self-contained contraction results are given that are used within the main proofs of the paper.
- Appendix C provides proofs for the results in Section 4 concerning the formation of the linear system that is solved by the DCFP algorithm, and verification that the derived system has the unique desired solution.
- Appendix D provides proofs relating to the stochastic categorical CDF Bellman equation, in particular establishing the desired unique solution to this new distributional Bellman equation, and proving a key bound on the local squared-Cramér variation that is used within the proof of the main theorem of the paper.
- Appendix E provides the proof of the main result of the paper, Theorem 5.1, giving full details for the steps traced through in the sketch proof in the main paper.
- Appendix F provides full details relating to the experiments in the main paper, as well as additional empirical comparisons between methods for distributional RL with a generative model.

A. Related work

Other families of model-based distributional RL algorithms. There are many approaches to distributional RL; important choices studied previously include moments (Sobel, 1982), exponential families (Morimura et al., 2010b), categorical distributions (Bellemare et al., 2017), collections of particles (Morimura et al., 2010a; Nguyen-Tang et al., 2021), quantiles (Dabney et al., 2018b), and generative models (Doan et al., 2018; Dabney et al., 2018a; Freirich et al., 2019; Yang et al., 2019; Yue et al., 2020). Our choice of categorical representations in this work is motivated by several considerations: (i) the existence of principled dynamic programming methods for these representations, with corresponding convergence theory (Rowland et al., 2018); (ii) the flexibility of these representations to trade-off computational complexity with accuracy (by varying m) (Rowland et al., 2018); (iii) the mathematical structure of the dynamic programming operator (linear), as described in this work; and (iv) the availability of an efficient algorithm to exactly compute the DP fixed point (the DCFP algorithm proposed in Section 4.1). An interesting and important direction, given our empirical findings in Section 6, is whether analyses can also be carried out for other approaches to distributional dynamic programming, such as quantile dynamic programming (QDP; Dabney et al., 2018b; Rowland et al., 2023; Bellemare et al., 2023), and fitted likelihood estimation (FLE; Wu et al., 2023). We expect challenges in extending the analysis to result due to the fact that, for example, the QDP operator is non-linear, and FLE operator applications typically do not have closed forms. Nevertheless, it would be particularly interesting to understand whether it is possible to obtain instance-dependent bounds for QDP, particularly given its strong empirical performance. Similarly, as described in Section 5, an interesting question for future work is whether it is possible to improve on the computational complexity of model-based DCFP for high-probability return-direction estimation.

Other statistical questions in distributional RL. Böck & Heirzinger (2022) propose a *model-free* algorithm for distributional RL, speedy categorical TD-learning, motivated by categorical TD learning (Rowland et al., 2018) and speedy Q-learning (Azar et al., 2011), and prove a sample complexity bound of $\tilde{O}(\varepsilon^{-2}(1-\gamma)^{-3})$ for high probability ε -accurate estimation in Cramér distance (which implies a non-minimax sample complexity of $\tilde{O}(\varepsilon^{-2}(1-\gamma)^{-4})$ in Wasserstein-1 distance, per Lemma 5.2). Wu et al. (2023) study the offline evaluation problem, in which state-action pairs are sampled from the stationary distribution of the policy, via fitted likelihood estimation (FLE) and focus on generalisation bounds, allowing for policy evaluation in environments with uncountable state spaces. Wang et al. (2023c) also study policy evaluation in this context, focusing on the LQR model. Aside from studying minimax optimality, Zhang et al. (2023) also make several other contributions on the topic of statistical efficiency of estimation for distributional RL, including analysis of asymptotic fluctuations and limit theorems, and analysis of approximations in more general metrics, including Wasserstein- p , Kolmogorov-Smirnov, and total variation metrics. Their sample complexity results rely on careful analysis of the behaviour of the *unprojected* distributional Bellman operator \mathcal{T} on certain subspaces of probability/signed measures.

Sample complexity of mean-return estimation. The sample complexity of estimating mean returns, and the related task of obtaining a near-optimal policy, has been considered by Azar et al. (2013); Sidford et al. (2018); Pananjady & Wainwright

(2020); Agarwal et al. (2020); Li et al. (2020). Interestingly, Agarwal et al. (2020), while treating the mean-return case, make use of return-binning as a proof technique. Li et al. (2020) also obtain bounds for mean-return sample complexity that apply with $\varepsilon > (1 - \gamma)^{-1/2}$ for modifications of certainty-equivalent model-based algorithms; an interesting direction for future work would be to check whether the restrictions on ε in Theorem 5.1 can be lifted by incorporating ideas from this mean-return analysis to the distributional setting. Additionally, Chandak et al. (2021) consider the task of estimating the variance of returns from off-policy data, and Wang et al. (2023b) study regret minimisation properties (with respect to the expected return criterion) of distributional RL algorithms in the online setting.

Further analysis. In this paper, we have resolved a conjecture of Zhang et al. (2023), obtaining a near-minimax-optimal algorithm for estimation of return distributions in Wasserstein-1 distance. Zhang et al. (2023) make contributions to several other important statistical questions regarding distributional RL, including approximation in stronger metrics such as Kolmogorov-Smirnov and total variation metrics, as well as studying asymptotic fluctuations of estimators; it will be interesting to see whether the analysis presented here can be extended to these other settings as well.

B. Additional CDF operator notation and contractivity results

In this section, we introduce finer-grained notation for the CDF operator T_P that allows us to straightforwardly refer to the operations that correspond to shifting/scaling/projecting, and to mixing over transition states, separately. We also establish several additional contraction lemmas that will be useful in the sections that follow.

B.1. Categorical hat function definition

For convenience, we provide the full mathematical definition of the hat functions $h_i : [0, (1 - \gamma)^{-1}] \rightarrow [0, 1]$ used in defining the categorical projection described in the main paper, as given by Rowland et al. (2018). For $i = 2, \dots, m - 1$, we have

$$h_i(z) = \begin{cases} \frac{z - z_{i-1}}{z_i - z_{i-1}} & \text{for } z \in [z_{i-1}, z_i] \\ \frac{z_{i+1} - z}{z_{i+1} - z_i} & \text{for } z \in [z_i, z_{i+1}] \\ 0 & \text{otherwise.} \end{cases}$$

For the edge case h_1 , we have

$$h_1(z) = \begin{cases} \frac{z_2 - z}{z_2 - z_1} & \text{for } z \in [z_1, z_2] \\ 0 & \text{otherwise,} \end{cases}$$

and similarly for the edge case h_m , we have

$$h_m(z) = \begin{cases} \frac{z - z_{m-1}}{z_m - z_{m-1}} & \text{for } z \in [z_{m-1}, z_m] \\ 0 & \text{otherwise.} \end{cases}$$

B.2. Finer-grained operator expression

Recall that the CDF operator $T_P : \mathbb{R}^{\mathcal{X} \times m} \rightarrow \mathbb{R}^{\mathcal{X} \times m}$ is represented by a matrix with elements given by

$$T_P(x, i; j, y) = P(y|x)(H_{i,j}^x - H_{i,j+1}^x). \quad (17)$$

We can therefore conceptualise the application $T_P F$ as standard matrix-vector multiplication in the vector space $\mathbb{R}^{\mathcal{X} \times m}$. However, the expression for matrix elements in Equation (17) has additional structure that means we can express the application of T_P in a different manner, which will be convenient in several proofs below, particularly as it separates out the influence of rewards (which remain fixed) and transition dynamics (which are estimated via samples).

In particular, we will regard $F \in \mathbb{R}^{\mathcal{X} \times m}$ itself as a matrix, with rows indexed by states in \mathcal{X} , and columns indexed by indices $i = 1, \dots, m$. For each state $x \in \mathcal{X}$, we then introduce the matrix $B_x \in \mathbb{R}^{m \times m}$, with (i, j) element given by

$$H_{i,j}^x - H_{i,j+1}^x.$$

We then have that $(T_P F)(x) \in \mathbb{R}^m$ can alternatively be expressed in matrix notation as

$$P_x F B_x^\top,$$

where P_x is the row vector given by the row of P corresponding to state $x \in \mathcal{X}$.

B.3. Additional results

Below, we provide several additional results regarding contractivity properties of T_P . To do so, it is useful to introduce the norm $\|\cdot\|_{\ell_2}$ on \mathbb{R}^m , which we define by

$$\|F\|_{\ell_2} = \left[\frac{1}{m(1-\gamma)} \sum_{i=1}^m F_i(x)^2 \right]^{1/2}.$$

The motivation for this definition is that if we have two distributions $\nu, \nu' \in \mathcal{P}(\{z_1, \dots, z_m\})$ with corresponding CDF vectors $F, F' \in \mathbb{R}^m$, then $\ell_2(\nu, \nu') = \|F - F'\|_{\ell_2}$, as ν, ν' are supported on $[0, (1-\gamma)^{-1}]$. Thus, under the abuse of notation $\ell_2(F, F')$ introduced in the main paper, we have $\ell_2(F, F') = \|F - F'\|_{\ell_2}$. We also introduce a supremum version of this norm on the space $\mathbb{R}^{\mathcal{X} \times m}$, which we denote by $\|\cdot\|_{\ell_2, \infty}$, and define by

$$\|F\|_{\ell_2, \infty} = \max_{x \in \mathcal{X}} \|F(x)\|_{\ell_2},$$

for all $F \in \mathbb{R}^{\mathcal{X} \times m}$. This norm is defined so that if we have RDFs $\eta, \eta' \in \mathcal{P}(\{z_1, \dots, z_m\})^{\mathcal{X}}$, and $F, F' \in \mathbb{R}^{\mathcal{X} \times m}$ are the corresponding CDF values, then

$$\bar{\ell}_2(\eta, \eta') = \|F - F'\|_{\ell_2, \infty}.$$

With this norm defined, we can now state and prove our first result, which essentially translates the contraction result in Proposition 2.2, expressed purely in terms of probability distributions and the Cramér distance ℓ_2 , into a slightly more general result expressed over $\mathbb{R}^{\mathcal{X} \times m}$ and the norm $\|\cdot\|_{\ell_2}$.

Proposition B.1. *The operator $T_P : \mathbb{R}^{\mathcal{X} \times m} \rightarrow \mathbb{R}^{\mathcal{X} \times m}$ is a contraction when restricted to the subspace $\{F \in \mathbb{R}^{\mathcal{X} \times m} : F_m(x) = 0 \text{ for all } x \in \mathcal{X}\}$ with respect to the norm $\|\cdot\|_{\ell_2, \infty}$, with contraction factor $\sqrt{\gamma}$.*

Proof. By Proposition 2.2, for any two RDF approximations $\eta, \eta' \in \mathcal{P}(\{z_1, \dots, z_m\})^{\mathcal{X}}$ with corresponding CDF values $F, F' \in \mathbb{R}^{\mathcal{X}}$, we have

$$\bar{\ell}_2(\Pi_m \mathcal{T} \eta, \Pi_m \mathcal{T} \eta') \leq \sqrt{\gamma} \bar{\ell}_2(\eta, \eta'),$$

and hence we also have

$$\|T_P F - T_P F'\|_{\ell_2, \infty} \leq \sqrt{\gamma} \|F - F'\|_{\ell_2, \infty}.$$

Hence, T_P is a contraction map on the set

$$\{F - F' : 0 \leq F_1(x) \leq \dots \leq F_m(x) = 1, 0 \leq F'_1(x) \leq \dots \leq F'_m(x) = 1 \text{ for all } x \in \mathcal{X}\}.$$

This set contains a basis for the subspace $\{F \in \mathbb{R}^{\mathcal{X} \times m} : F_m(x) = 0 \text{ for all } x \in \mathcal{X}\}$. Namely, the one-hot vector at coordinate (x, j) (for $j < m$) can be exhibited as lying in this subspace since it can be expressed as the difference between the vectors $F, F' \in \mathbb{R}^{\mathcal{X} \times m}$ defined by $F_j(y) = F'_j(y) = 1$ for all $y \neq x$, and all $j = 1, \dots, m$, and $F_i(x) = 1$ for $i \geq j$ (and 0 otherwise), and $F'_i(x) = 1$ for $i \geq j + 1$ (and 0 otherwise). Since T_P is linear, it therefore holds that

$$\|T_P F\|_{\ell_2, \infty} \leq \sqrt{\gamma} \|F\|_{\ell_2, \infty}, \quad (18)$$

for any F in the subspace $\{F \in \mathbb{R}^{\mathcal{X} \times m} : F_m(x) = 0 \text{ for all } x \in \mathcal{X}\}$, as required. \square

Proposition B.2. *For each $x \in \mathcal{X}$, the matrix B_x is a contraction mapping on the space $\{F \in \mathbb{R}^m : F_m = 0\}$ with respect to $\|\cdot\|_{\ell_2}$, with contraction factor $\sqrt{\gamma}$.*

Proof. Consider a related one-state MRP, for which the reward at the single state is $r(x)$, and the state transitions to itself with probability 1. The categorical Bellman operator associated with this MRP and the support $\{z_1, \dots, z_m\}$ is precisely B_x , and the statement of the result therefore follows as a special case of Proposition B.1. \square

The next result serves as a counterpoint to Proposition B.2; it shows that if m is sufficiently large, the map B_x does not contract by too much in $\|\cdot\|_{\ell_2}$.

Proposition B.3. For any $F, F' \in \mathcal{F}$, we have

$$\|B_x F - B_x F'\|_{\ell_2}^2 \geq \gamma \|F - F'\|_{\ell_2}^2 - \frac{2}{m(1-\gamma)^{1/2}} - \frac{1}{m^2(1-\gamma)^2}.$$

This is proven via the following lemma.

Lemma B.4. For any $\nu \in \mathcal{P}([0, (1-\gamma)^{-1}])$ and the projection $\Pi_m : \mathcal{P}([0, (1-\gamma)^{-1}]) \rightarrow \mathcal{P}(\{z_1, \dots, z_m\})$, we have

$$\ell_2(\nu, \Pi_m \nu) \leq \frac{1}{2\sqrt{m(1-\gamma)}},$$

Further, for any $\nu, \nu' \in \mathcal{P}([0, (1-\gamma)^{-1}])$, we have

$$\ell_2(\Pi_m \nu, \Pi_m \nu') \geq \ell_2(\nu, \nu') - \frac{1}{m(1-\gamma)},$$

and

$$\ell_2^2(\Pi_m \nu, \Pi_m \nu') \geq \ell_2^2(\nu, \nu') - \frac{2}{m(1-\gamma)^{1/2}} - \frac{1}{m^2(1-\gamma)^2}.$$

Proof. By Rowland et al. (2018, Proposition 6), we have that the CDF values $F_{\Pi_m \nu}(z_i)$ for $i = 1, \dots, m-1$ are equal to the average of the CDF values of F_ν on the interval $[z_i, z_{i+1}]$. Therefore, in computing the squared Cramér distance $\ell_2^2(\nu, \Pi_m \nu)$, the worst-case contribution to the integral

$$\ell_2^2(\nu, \Pi_m \nu) = \int_0^{(1-\gamma)^{-1}} (F_\nu(t) - F_{\Pi_m \nu}(t))^2 dt$$

from the interval $[z_i, z_{i+1}]$, holding $F_\nu(z_i)$ and $F_\nu(z_{i+1})$ constant, is

$$(z_{i+1} - z_i) \left(\frac{F(z_{i+1}) - F(z_i)}{2} \right)^2 = \frac{1}{4m(1-\gamma)} (F(z_{i+1}) - F(z_i))^2.$$

Thus, the worst-case value for the entire integral is

$$\frac{1}{4m(1-\gamma)} \sum_{i=1}^{m-1} (F(z_i) - F(z_{i+1}))^2.$$

The worst-case value for the sum is 1, by interpreting this as a sum of squared probabilities, and we therefore deduce that

$$\ell_2^2(\nu, \Pi_m \nu) \leq \frac{1}{4m(1-\gamma)},$$

leading to

$$\ell_2(\nu, \Pi_m \nu) \leq \frac{1}{2\sqrt{m(1-\gamma)}},$$

as required for the first stated inequality. For the second and third inequalities, we apply the triangle inequality twice to obtain

$$\ell_2(\nu, \nu') \leq \ell_2(\nu, \Pi_m \nu) + \ell_2(\Pi_m \nu, \Pi_m \nu') + \ell_2(\Pi_m \nu', \nu') \leq \ell_2(\Pi_m \nu, \Pi_m \nu') + \frac{1}{m(1-\gamma)};$$

rearrangement then gives the second statement. Squaring both sides of the inequality above gives

$$\ell_2^2(\nu, \nu') \leq \ell_2^2(\Pi_m \nu, \Pi_m \nu') + \frac{2}{m(1-\gamma)} \ell_2(\Pi_m \nu, \Pi_m \nu') + \frac{1}{m^2(1-\gamma)^2}.$$

Bounding the instance of $\ell_2(\Pi_m \nu, \Pi_m \nu')$ in the cross-term on the right-hand side by $(1-\gamma)^{1/2}$ and rearranging then yields the result. \square

Proof of Proposition B.3. Let $\nu, \nu' \in \mathcal{P}(\{z_1, \dots, z_m\})$ be the distributions with CDF values F, F' , respectively, and let G, G' be random variables with CDFs F, F' respectively, and (x, X') an independent random transition in the MRP beginning at state x . Recall from the notation introduced earlier in this section that $B_x F$ and $B_x F'$ are the CDF values of the distributions of $r(x) + \gamma G$ and $r(x) + \gamma G'$ after projection onto the support grid $\{z_1, \dots, z_m\}$ by the projection map Π_m . Following common notation in distributional RL (Bellemare et al., 2023), we denote the distributions of $r(x) + \gamma G$ and $r(x) + \gamma G'$ by $(b_{r(x), \gamma})\#\nu$ and $(b_{r(x), \gamma})\#\nu'$, respectively. Here, $b_{r(x), \gamma} : \mathbb{R} \rightarrow \mathbb{R}$ is the bootstrap function $b_{r(x), \gamma}(z) = r(x) + \gamma z$, and $(b_{r(x), \gamma})\#\nu$ is the push-forward distribution of ν through $b_{r(x), \gamma}$ (intuitively, the distribution obtained by transforming the support of ν according to $b_{r(x), \gamma}$). With this notation introduced, we therefore have

$$\begin{aligned} \|B_x F - B_x F'\|_{\ell_2}^2 &= \ell_2^2(\Pi_m((b_{r(x), \gamma})\#\nu), \Pi_m((b_{r(x), \gamma})\#\nu')) \\ &\stackrel{(a)}{\geq} \ell_2^2((b_{r(x), \gamma})\#\nu, (b_{r(x), \gamma})\#\nu') - \frac{2}{m(1-\gamma)^{1/2}} - \frac{1}{m^2(1-\gamma)^2} \\ &\stackrel{(b)}{=} \gamma \ell_2^2(\nu, \nu') - \frac{2}{m(1-\gamma)^{1/2}} - \frac{1}{m^2(1-\gamma)^2} \\ &= \gamma \|F - F'\|_{\ell_2}^2 - \frac{2}{m(1-\gamma)^{1/2}} - \frac{1}{m^2(1-\gamma)^2}, \end{aligned}$$

as required, where (a) follows from Lemma B.4, and (b) follows from homogeneity of Cramér distance (see Rowland et al. (2018, Proof of Proposition 2)). \square

C. Proofs of results in Section 4

Proposition 4.1. *If $\eta \in \mathcal{P}(\{z_1, \dots, z_m\})^{\mathcal{X}}$ is an RDF with corresponding CDF values $F \in \mathbb{R}^{\mathcal{X} \times m}$, then the corresponding CDF values $F' \in \mathbb{R}^{\mathcal{X} \times m}$ for $\Pi_m \mathcal{T} \eta$ satisfy*

$$F'_i(x) = \sum_{y \in \mathcal{X}} \sum_{j=1}^m P(y|x) (H_{i,j}^x - H_{i,j+1}^x) F_j(y), \quad (7)$$

where

$$H_{i,j}^x = \sum_{l \leq i} h_l(r(x) + \gamma z_j) \quad (8)$$

for $j = 1, \dots, m$, and by convention we take $H_{i,m+1}^x = 0$.

Proof. Beginning by restating Equation (6), we have that if $\eta \in \mathcal{P}(\{z_1, \dots, z_m\})^{\mathcal{X}}$ is an RDF with corresponding probability mass values $p \in \mathbb{R}^{\mathcal{X} \times m}$, then the updated RDF $\eta' = \Pi_m \mathcal{T} \eta$ has corresponding probability mass values $p' \in \mathbb{R}^{\mathcal{X} \times m}$ given by

$$p'_i(x) = \sum_{y \in \mathcal{X}} \sum_{j=1}^m P(y|x) h_{i,j}^x p_j(y).$$

First, for $i \in \{1, \dots, m\}$, we sum l from 1 to i to yield

$$F'_i(x) = \sum_{l \leq i} p'_l(x) = \sum_{y \in \mathcal{X}} \sum_{j=1}^m P(y|x) \sum_{l \leq i} h_{l,j}^x p_j(y) = \sum_{y \in \mathcal{X}} \sum_{j=1}^m P(y|x) H_{i,j}^x p_j(y) = \sum_{y \in \mathcal{X}} \sum_{j=1}^m P(y|x) H_{i,j}^x (F_j(y) - F_{j-1}(y)),$$

where by convention we take $F_0(y) \equiv 0$. By reorganising the terms on the right-hand side, the claim now follows. \square

Proposition 4.2. *The linear system in Equation (10), with the additional linear constraints $F_m(x) = 1$ for all $x \in \mathcal{X}$, is equivalent to the following linear system in $\tilde{F} \in \mathbb{R}^{\mathcal{X} \times [m-1]}$:*

$$(I - \tilde{T}_P) \tilde{F} = \tilde{H}, \quad (11)$$

where the $(x, i; y, j)$ coordinate of \tilde{T}_P (for $1 \leq i, j \leq m-1$) is

$$\tilde{T}_P(x, i; y, j) = P(y|x) (H_{i,j}^x - H_{i,j+1}^x),$$

and for each $x \in \mathcal{X}$, $1 \leq i \leq m - 1$:

$$\tilde{H}(x, i) = H_{i,m}^x.$$

Proof. First, we consider a row of $F = T_P F$ that corresponds to the index (x, i) , with $i \neq m$. Expanding under the definition of T_P , we have

$$F_i(x) = \sum_{y \in \mathcal{X}} \sum_{j=1}^{m-1} P(y|x)(H_{i,j}^x - H_{i,j+1}^x)F_j(y) + \sum_{y \in \mathcal{X}} P(y|x)H_{i,m}^x F_m(y).$$

Since we assume the additional constraints $F_m(y) \equiv 1$ for all $y \in \mathcal{X}$, the final term on the right-hand side can be simplified to yield

$$F_i(x) = \sum_{y \in \mathcal{X}} \sum_{j=1}^{m-1} P(y|x)(H_{i,j}^x - H_{i,j+1}^x)F_j(y) + H_{i,m}^x.$$

This is precisely the row of $\tilde{F} = \tilde{T}_P \tilde{F} + \tilde{H}$ corresponding to index (x, i) .

Now, we consider a row of $F = T_P F$ that corresponds to the index (x, m) . Again making the substitution $F_m(y) \equiv 1$ for all $y \in \mathcal{X}$, we have

$$1 \equiv F_m(x) = \sum_y \sum_{j=1}^{m-1} P(y|x) \overbrace{(H_{m,j}^x - H_{m,j+1}^x)}^{=0} F_j(y) + \sum_y P(y|x)H_{m,m}^x F_m(y) = \sum_y P(y|x)H_{m,m}^x F_m(y) \equiv 1,$$

which shows that the equation is redundant, and hence can be removed from the system. The claim $H_{m,j}^x - H_{m,j+1}^x = 0$ follows since in fact $H_{m,j}^x = \sum_{i=1}^m h_i(r(x) + \gamma z_j)$, and the sum over the hat functions for any input argument is 1. In the final equality, we have used the fact that $H_{m,m}^x = 1$ similarly. Thus, we have deduced the claim of the proposition. \square

Proposition 4.3. *The linear system in Equation (11) has a unique solution, which is precisely the CDF values $((F_i^*(x))_{i=1}^{m-1}) : x \in \mathcal{X}$ of the categorical fixed point.*

Proof. By Proposition 4.2, we have that the CDF values \tilde{F}^* of the categorical fixed-point solve Equation (11). Now, let us suppose that \tilde{F}_1, \tilde{F}_2 are distinct solutions to Equation (11), aiming to obtain a contradiction. Proposition 4.2 also establishes that Equation (11) is equivalent to Equation (10) with the additional conditions that $F_m(x) = 1$ for all $x \in \mathcal{X}$, so we will denote the corresponding two solutions to Equation (10) built from \tilde{F}_1, \tilde{F}_2 (by setting the unspecified (x, m) coordinates to 1) by F_1, F_2 , respectively.

The idea is now to use the contractivity of the projected operator $\Pi_m \mathcal{T}$ in ℓ_2 , as established in Proposition 2.2, to obtain a contradiction. Notationally, it is useful to phrase things in terms of contractivity of the CDF operator T_P itself. We use the norms $\|\cdot\|_{\ell_2}$ and $\|\cdot\|_{\ell_2, \infty}$, defined on \mathbb{R}^m and $\mathbb{R}^{\mathcal{X} \times m}$ in Appendix B, which we recall here for convenience:

$$\|F\|_{\ell_2} = \left[\frac{1}{m(1-\gamma)} \sum_{i=1}^m F_i^2 \right]^{1/2} \quad \text{for } F \in \mathbb{R}^m, \quad \text{and} \quad \|F\|_{\ell_2, \infty} = \max_{x \in \mathcal{X}} \|F(x)\|_{\ell_2} \quad \text{for } F \in \mathbb{R}^{\mathcal{X} \times m}$$

We therefore have

$$\|T_P(F_1 - F_2)\|_{\ell_2, \infty} = \|T_P F_1 - T_P F_2\|_{\ell_2, \infty} = \|F_1 - F_2\|_{\ell_2, \infty}.$$

However, Proposition B.1 establishes that T_P is a contraction on $\{F \in \mathbb{R}^{\mathcal{X} \times m} : F_m(x) = 0 \text{ for all } x \in \mathcal{X}\}$ with respect to $\|\cdot\|_{\ell_2, \infty}$, which contradicts the statement above, as required. \square

D. Proofs relating to the stochastic CDF Bellman equation

Before giving the proofs, we present a version of the SC-CDF Bellman equation in a purely distributional form, which will streamline the arguments. This mirrors the development of the form of the distributional Bellman equation given purely in terms of distributions (Rowland et al., 2018), rather than in random variable form as in Bellemare et al. (2017). We define the stochastic categorical CDF Bellman operator $\mathcal{T}_{\text{SCC}} : \mathcal{P}(\mathcal{F})^{\mathcal{X}} \rightarrow \mathcal{P}(\mathcal{F})^{\mathcal{X}}$ for each $\psi \in \mathcal{P}(\mathcal{F})^{\mathcal{X}}$ by

$$(\mathcal{T}_{\text{SCC}} \psi)(x) = \mathcal{D}((\hat{T}_P \Phi)(x)),$$

where $\Phi(y) \sim \psi(y)$ independently of \hat{T}_P , and \mathcal{D} extracts the distribution of the input random variable. The purely distributional form of the SC-CDF Bellman equation is then written as a fixed point condition on $\mathcal{P}(\mathcal{F})^{\mathcal{X}}$:

$$\psi = \mathcal{T}_{\text{SCC}} \psi. \quad (19)$$

We also write

$$\bar{w}_{\|\cdot\|_{\ell_2}}(\psi, \psi') = \max_{x \in \mathcal{X}} w_{\|\cdot\|_{\ell_2}}(\psi(x), \psi'(x))$$

for the supremum-Wasserstein distance over $\mathcal{P}(\mathcal{F})^{\mathcal{X}}$ with base metric $\|\cdot\|_{\ell_2}$ on \mathcal{F} .

Proposition 5.7. *The SC-CDF Bellman equation in Equation (16) has a unique solution, in the sense that there is a unique distribution for each $\Phi(x)$ such that Equation (16) holds for each $x \in \mathcal{X}$.*

Proof. We first show that the operator \mathcal{T}_{SCC} is a contraction on $\mathcal{P}(\mathcal{F})^{\mathcal{X}}$ with respect to the metric $\bar{w}_{\|\cdot\|_{\ell_2}}$. Suppose $\psi, \psi' \in \mathcal{P}(\mathcal{F})^{\mathcal{X}}$, and let $(\Phi(y), \Phi'(y))$ be an optimal coupling between $\psi(y)$ and $\psi'(y)$ with respect to $w_{\|\cdot\|_{\ell_2}}$ for each $y \in \mathcal{X}$ (existence of such couplings is guaranteed by Villani (2009, Theorem 4.1)). Then, letting (x, X') be a random transition from x , independent of Φ, Φ' , we have that $(B_x \Phi(X'), B_x \Phi'(X'))$ is a valid coupling of $(\mathcal{T}_{\text{SCC}} \psi)(x)$ and $(\mathcal{T}_{\text{SCC}} \psi')(x)$. Then we have, using the operator notation defined in Appendix B,

$$\begin{aligned} w_{\|\cdot\|_{\ell_2}}((\mathcal{T}_{\text{SCC}} \psi)(x), (\mathcal{T}_{\text{SCC}} \psi')(x)) &\stackrel{(a)}{\leq} \mathbb{E} \left[\|B_x \Phi(X') - B_x \Phi'(X')\|_{\ell_2} \right] \\ &\stackrel{(b)}{\leq} \sqrt{\gamma} \mathbb{E} \left[\|\Phi(X') - \Phi'(X')\|_{\ell_2} \right] \\ &= \sqrt{\gamma} \sum_{y \in \mathcal{X}} P(y|x) \mathbb{E} \left[\|\Phi(y) - \Phi'(y)\|_{\ell_2} \right] \\ &\stackrel{(c)}{=} \sqrt{\gamma} \sum_{y \in \mathcal{X}} P(y|x) w_{\|\cdot\|_{\ell_2}}(\psi(y), \psi'(y)) \\ &\leq \sqrt{\gamma} \bar{w}_{\|\cdot\|_{\ell_2}}(\psi, \psi'), \end{aligned}$$

where (a) follows since $(B_x \Phi(X'), B_x \Phi'(X'))$ is a valid coupling of $(\mathcal{T}_{\text{SCC}} \psi)(x)$ and $(\mathcal{T}_{\text{SCC}} \psi')(x)$, (b) follows by contractivity of B_x with respect to $\|\cdot\|_{\ell_2}$, as shown in Proposition B.2, and (c) follows since $(\Phi(y), \Phi'(y))$ was chosen to be an optimal coupling of $\psi(y)$ and $\psi'(y)$. Hence we have

$$\bar{w}_{\|\cdot\|_{\ell_2}}(\mathcal{T}_{\text{SCC}} \psi, \mathcal{T}_{\text{SCC}} \psi') \leq \sqrt{\gamma} \bar{w}_{\|\cdot\|_{\ell_2}}(\psi, \psi'),$$

proving contractivity.

The metric space $(\mathcal{P}(\mathcal{F})^{\mathcal{X}}, \bar{w}_{\|\cdot\|_{\ell_2}})$ is complete, since the base space $(\mathcal{F}, \|\cdot\|_{\ell_2})$ is separable and complete (Villani, 2009, Theorem 6.18). Hence, by Banach's fixed point theorem, we obtain that there is a unique fixed point $\psi^* \in \mathcal{P}(\mathcal{F})^{\mathcal{X}}$ of \mathcal{T}_{SCC} . Thus, a collection of random CDFs $(\Phi^*(x) : x \in \mathcal{X})$ satisfy the SC-CDF Bellman equation in Equation (16) if and only if we have $\Phi^*(x) \sim \psi^*(x)$ for all $x \in \mathcal{X}$. \square

Proposition 5.8. *We have $\mathbb{E}[\Phi^Q(x)] = F^Q(x)$ for all $x \in \mathcal{X}$.*

Proof. We take expectations on both sides of the random-variable stochastic categorical CDF Bellman equation in Equation (16), yielding:

$$\mathbb{E}[\Phi^Q(x)] = \mathbb{E}[(\hat{T}_Q \Phi^Q)(x)].$$

Since \hat{T}_Q is a random linear map, independent of Φ^Q , we have

$$\begin{aligned} \mathbb{E}[\Phi^Q(x)] &= (\mathbb{E}[\hat{T}_Q] \mathbb{E}[\Phi^Q])(x) \\ &= T_Q \mathbb{E}[\Phi^Q](x). \end{aligned}$$

This states that $\mathbb{E}[\Phi^Q] \in \mathbb{R}^{\mathcal{X} \times m}$ satisfies the standard categorical Bellman equation in Equation (10), and hence $\mathbb{E}[\Phi^Q] = F^Q$, by Proposition 2.2, as required. \square

Proposition 5.11. *We have*

$$\Sigma_Q \geq \sigma_Q + \gamma Q \Sigma_Q - \left(\frac{2}{m\sqrt{1-\gamma}} + \frac{1}{m^2(1-\gamma)^2} \right) \mathbf{1},$$

where $\mathbf{1} \in \mathbb{R}^{\mathcal{X}}$ is a vector of ones, and the inequality above is interpreted component-wise.

Proof. We calculate, writing Φ^Q as Φ , F^Q as F , and \hat{T}_Q as \hat{T} to lighten notation:

$$\begin{aligned} \Sigma_Q(x) &= \mathbb{E}[\ell_2^2(\Phi(x), F(x))] \\ &\stackrel{(a)}{=} \mathbb{E}[\ell_2^2((\hat{T}\Phi)(x), F(x))] \\ &\stackrel{(b)}{=} \mathbb{E}[\ell_2^2((\hat{T}F)(x), F(x))] + \mathbb{E}[\ell_2^2((\hat{T}\Phi)(x), (\hat{T}F)(x))]. \end{aligned} \quad (20)$$

Here, (a) follows since Φ satisfies the random-variable version of the stochastic categorical CDF Bellman equation, (b) is a result of a Pythagorean identity for squared Cramér distance, which we derive below:

$$\begin{aligned} \mathbb{E}[\ell_2^2((\hat{T}\Phi)(x), F(x))] &= \mathbb{E} \left[\int_0^{(1-\gamma)^{-1}} ((\hat{T}\Phi)(x)(t) - F(x)(t))^2 dt \right] \\ &= \int_0^{(1-\gamma)^{-1}} \mathbb{E}[(\hat{T}\Phi)(x)(t) - F(x)(t)]^2 dt, \end{aligned}$$

where the integral switch follows from Fubini's theorem. Now, focusing on the integrand above, it can be written as

$$\mathbb{E}[(Y - \mathbb{E}[Y])^2]$$

with $Y = (\hat{T}\Phi)(x)(t)$, since $F(x) = \mathbb{E}[(\hat{T}\Phi)(x)] = \mathbb{E}[\Phi(x)]$, by Lemma 5.8. We have

$$\begin{aligned} \mathbb{E}[(Y - \mathbb{E}[Y])^2] &= \mathbb{E}[(Y - \mathbb{E}[Y|\hat{T}] + \mathbb{E}[Y|\hat{T}] - \mathbb{E}[Y])^2] \\ &= \mathbb{E}[(Y - \mathbb{E}[Y|\hat{T}])^2] + \mathbb{E}[(\mathbb{E}[Y|\hat{T}] - \mathbb{E}[Y])^2]. \end{aligned}$$

Now, $\mathbb{E}[(\hat{T}\Phi)(x)(t) | \hat{T}] = (\hat{T}\mathbb{E}[\Phi])(x)(t) = (\hat{T}F)(x)(t)$, by linearity, which concludes the validation of step (b) above. We recognise the first term in Equation (20) as the local squared-Cramér variation, and hence have

$$\Sigma_Q(x) = \sigma_Q(x) + \mathbb{E}[\ell_2^2((\hat{T}\Phi)(x), (\hat{T}F)(x))].$$

We now explicitly write the evaluation of the application of \hat{T} at coordinate x in terms of the random transition (x, X') used to construct the single-sample random transition matrix \hat{Q} described in Definition 5.4, so that we obtain, with the operator

notation of Appendix B,

$$\begin{aligned}
 \mathbb{E}[\ell_2^2((\hat{T}\Phi)(x), (\hat{T}F)(x))] &= \mathbb{E}[\ell_2^2(B_x\Phi(X'), B_xF(X'))] \\
 &= \mathbb{E}[\mathbb{E}[\ell_2^2(B_x\Phi(X'), B_xF(X')) \mid \Phi]] \\
 &= \mathbb{E}\left[\sum_{y \in \mathcal{X}} Q(y|x) \ell_2^2(B_x\Phi(y), B_xF(y))\right] \\
 &\stackrel{(a)}{\geq} \sum_{y \in \mathcal{X}} Q(y|x) \mathbb{E}[\gamma \ell_2^2(\Phi(y), F(y)) - \alpha] \\
 &= \gamma \sum_{y \in \mathcal{X}} Q(y|x) \mathbb{E}[\ell_2^2(\Phi(y), F(y))] - \alpha \\
 &= \gamma \sum_{y \in \mathcal{X}} Q(y|x) \mathbb{E}[\ell_2^2(\Phi(y), F(y))] - \alpha \\
 &= \gamma(Q\Sigma_Q)(x) - \alpha,
 \end{aligned}$$

where (a) follows from Proposition B.3, with $\alpha = \frac{2}{m(1-\gamma)^{1/2}} + \frac{1}{m^2(1-\gamma)^2}$, meaning that we deduce

$$\Sigma_Q(x) = \sigma_Q(x) + \gamma(Q\Sigma_Q)(x) - \alpha,$$

as required. \square

Corollary 5.12. *We can bound the term $\|(I - \gamma\hat{P})^{-1}\sigma_{\hat{P}}\|_\infty$ appearing in Equation (14) under the assumptions of Theorem 5.3 as follows:*

$$\|(I - \gamma\hat{P})^{-1}\sigma_{\hat{P}}\|_\infty \leq \|\Sigma_{\hat{P}}\|_\infty + \frac{1}{1-\gamma} \leq \frac{2}{1-\gamma}.$$

Proof. By Proposition 5.11 applied with $Q = \hat{P}$,

$$\Sigma_{\hat{P}} \geq \sigma_{\hat{P}} + \gamma\hat{P}\Sigma_{\hat{P}} - \left(\frac{2}{m(1-\gamma)^{1/2}} + \frac{1}{m^2(1-\gamma)^2}\right)\mathbf{1},$$

where $\mathbf{1} \in \mathbb{R}^{\mathcal{X}}$ is the vector of ones. We first note that from the condition $m \geq 4\varepsilon^{-2}(1-\gamma)^{-2} + 1$ from the statement of Theorem 5.3, we have

$$\frac{2}{m(1-\gamma)^{1/2}} + \frac{1}{m^2(1-\gamma)^2} \leq \frac{2}{4\varepsilon^{-2}(1-\gamma)^{-2}(1-\gamma)^{1/2}} + \frac{1}{4\varepsilon^{-2}} \leq \frac{\varepsilon^2(1-\gamma)^{3/2}}{2} + \frac{\varepsilon^2}{4} < 1,$$

since $\varepsilon \in (0, 1)$, from the statement of Theorem 5.3.

We therefore have

$$(I - \gamma\hat{P})\Sigma_{\hat{P}} \geq \sigma_{\hat{P}} - \mathbf{1}.$$

Now, $(I - \gamma\hat{P})^{-1}$ is a monotone operator (in the sense that $v_1 \geq v_2$ coordinatewise implies $(I - \gamma\hat{P})^{-1}v_1 \geq (I - \gamma\hat{P})^{-1}v_2$; this claim follows as all elements of $(I - \gamma\hat{P})^{-1}$ are non-negative, since it can also be written $\sum_{k \geq 0} \gamma^k \hat{P}^k$), we can apply it to both sides of the inequality above to obtain

$$\Sigma_{\hat{P}} + (1-\gamma)^{-1}\mathbf{1} \geq (I - \gamma\hat{P})^{-1}\sigma_{\hat{P}}.$$

Finally, we note that since $\Sigma_{\hat{P}}(x)$ is an expected squared-Cramér distance between two CDFs supported on an interval of length $(1-\gamma)^{-1}$, we have

$$\Sigma_{\hat{P}}(x) \leq (1-\gamma)^{-1},$$

from which the claim follows. \square

E. Proof of Theorem 5.1

We begin by restating the result we seek to prove.

Theorem 5.1. *Let $\varepsilon \in (0, (1-\gamma)^{-1/2})$ and $\delta \in (0, 1)$, and suppose the number of categories satisfies $m \geq 4(1-\gamma)^{-2}\varepsilon^{-2} + 1$. Then the output \hat{F} of model-based DCFP with $N = \Omega(\varepsilon^{-2}(1-\gamma)^{-3}\text{polylog}(|\mathcal{X}|/\delta))$ samples satisfies*

$$\max_{x \in \mathcal{X}} w_1(\eta^*(x), \hat{F}(x)) \leq \varepsilon,$$

with probability at least $1 - \delta$.

We arrange the proof into a sequence of smaller results, in analogy with the presentation of the sketch proof in the main paper.

E.1. Reduction to high-probability bounds in Cramér distance

Following the sketch provided in the main paper, we first restate and prove Lemma 5.2.

Lemma 5.2. *For any two distributions $\nu, \nu' \in \mathcal{P}([0, (1-\gamma)^{-1}])$, we have*

$$w_1(\nu, \nu') \leq (1-\gamma)^{-1/2} \ell_2(\nu, \nu').$$

Proof. We begin by writing

$$w_1(\nu, \nu') = \int_0^{(1-\gamma)^{-1}} |F_\nu(t) - F_{\nu'}(t)| dt = (1-\gamma)^{-1} \left[(1-\gamma) \int_0^{(1-\gamma)^{-1}} |F_\nu(t) - F_{\nu'}(t)| dt \right],$$

where $F_\nu, F_{\nu'}$ are the CDFs of ν, ν' , respectively. The quantity inside the squared brackets can be interpreted as an expectation (with t ranging over the values of a uniform variate on $\mathbb{E}_{T \sim \text{Unif}([0, (1-\gamma)^{-1}])} [|F_\nu(T) - F_{\nu'}(T)|]$), and we can therefore apply Jensen's inequality with the map $z \mapsto z^2$. This then yields

$$\begin{aligned} w_1(\nu, \nu') &\leq (1-\gamma)^{-1} \left[(1-\gamma) \int_0^{(1-\gamma)^{-1}} (F_\nu(t) - F_{\nu'}(t))^2 dt \right]^{1/2} \\ &= (1-\gamma)^{-1/2} \ell_2(\nu, \nu'), \end{aligned}$$

as required. \square

The first main step of the proof of Theorem 5.1 is a reduction to Theorem 5.3 via Lemma 5.2. To see this, we first restate Theorem 5.3 here for convenience.

Theorem 5.3. *Let $\varepsilon \in (0, 1)$ and $\delta \in (0, 1)$, and suppose the number of categories satisfies $m \geq 4(1-\gamma)^{-2}\varepsilon^{-2} + 1$. Then the output \hat{F} of model-based DCFP with $N = \Omega(\varepsilon^{-2}(1-\gamma)^{-2}\text{polylog}(|\mathcal{X}|/\delta))$ samples satisfies*

$$\max_{x \in \mathcal{X}} \ell_2(\eta^*(x), \hat{F}(x)) \leq \varepsilon, \tag{13}$$

with probability at least $1 - \delta$.

For the proof of the reduction, suppose the statement of Theorem 5.3 holds. Now, let us take $\varepsilon \in (0, (1-\gamma)^{-1/2})$, and $m \geq 4(1-\gamma)^{-2}\varepsilon^{-2} + 1$, as in the assumptions of Theorem 5.1. We then define $\tilde{\varepsilon} = (1-\gamma)^{1/2}\varepsilon$; note that from the assumption on ε , we have $\tilde{\varepsilon} \in (0, 1)$. Applying the result of Theorem 5.3, we therefore obtain that with $N = \tilde{\Omega}(\tilde{\varepsilon}^{-2}(1-\gamma)^{-2}\text{polylog}(|\mathcal{X}|/\delta))$, we have (with probability at least $1 - \delta$)

$$\max_{x \in \mathcal{X}} \ell_2(\eta^*(x), \hat{F}(x)) \leq \tilde{\varepsilon}.$$

By Lemma 5.2, we therefore have (with probability at least $1 - \delta$, for all $x \in \mathcal{X}$)

$$\bar{w}_1(\eta^*(x), \hat{F}(x)) \leq (1-\gamma)^{-1/2} \ell_2(\eta^*(x), \hat{F}(x)) \leq (1-\gamma)^{-1/2} (1-\gamma)^{1/2} \varepsilon = \varepsilon,$$

which is the desired inequality in Theorem 5.1. Finally, we note that the sample complexity term $\tilde{\varepsilon}^{-2}(1-\gamma)^{-2}$ can be rewritten as

$$\tilde{\varepsilon}^{-2}(1-\gamma)^{-2} = ((1-\gamma)^{1/2}\varepsilon)^{-2}(1-\gamma)^{-2} = \varepsilon^{-2}(1-\gamma)^{-3}.$$

Thus, we obtain the stated sample complexity in Theorem 5.1, and we have established that to prove Theorem 5.1, it is sufficient to prove Theorem 5.3.

E.2. Reduction to categorical fixed-point error

The first step of the proof of Theorem 5.3 is to show that with m taken sufficiently large (as described in the statement of Theorem 5.3), the Cramér distance between the true return distributions and the categorical fixed points is small, and it is therefore sufficient to focus solely on the sample-based error in estimating the categorical fixed point.

By applying the triangle inequality, we have

$$\begin{aligned} \bar{\ell}_2(\eta^*, \hat{F}) &\leq \bar{\ell}_2(\eta^*, F^*) + \bar{\ell}_2(F^*, \hat{F}) \\ &\stackrel{(a)}{\leq} \frac{1}{(1-\gamma)\sqrt{m-1}} + \bar{\ell}_2(F^*, \hat{F}) \\ &\stackrel{(b)}{\leq} \frac{\varepsilon}{2} + \bar{\ell}_2(F^*, \hat{F}), \end{aligned}$$

where (a) follows from the fixed-point approximation bound in Equation (5), which itself is the result of Proposition 2 of Rowland et al. (2018), and (b) follows from substituting the assumed inequality for m in the statement of Theorem 5.3. Thus, to establish that $\bar{\ell}_2(\eta^*, \hat{F})$ is bounded by ε with probability at least $1-\delta$, it suffices to show that

$$\bar{\ell}_2(F^*, \hat{F}) < \varepsilon/2,$$

with probability at least $1-\delta$, as claimed.

E.3. Propagation of local errors

To begin analysing $\bar{\ell}_2(F^*, \hat{F})$, we analyse the difference of vectors $\hat{F} - F^*$ directly. We proceed in an analogous manner to Azar et al. (2013) in the mean-return case, rearranging as follows:

$$\begin{aligned} \hat{F} - F^* &\stackrel{(a)}{=} T_{\hat{P}}\hat{F} - T_P F^* \\ &\stackrel{(b)}{=} T_{\hat{P}}\hat{F} - T_{\hat{P}}F^* + T_{\hat{P}}F^* - T_P F^* \\ \implies (I - T_{\hat{P}})(\hat{F} - F^*) &= (T_{\hat{P}} - T_P)F^*. \end{aligned} \tag{21}$$

Here, (a) follows since \hat{F}, F^* are fixed points of $T_{\hat{P}}, T_P$, respectively, (b) follows by adding and subtracting $T_{\hat{P}}F^*$, and the implication follows from straightforward rearrangement.

We would next like to rearrange Equation (21) to leave the term $\hat{F} - F^*$ on its own. This requires some care, in checking that the operator $(I - T_{\hat{P}})$ is invertible in an appropriate sense.

Lemma E.1. *The operator $I - T_{\hat{P}} : \mathbb{R}^{\mathcal{X} \times m} \rightarrow \mathbb{R}^{\mathcal{X} \times m}$ is invertible on the subspace $\{F \in \mathbb{R}^{\mathcal{X} \times m} : F_m(x) = 0 \text{ for all } x \in \mathcal{X}\}$, with inverse $\sum_{k \geq 0} T_{\hat{P}}^k$.*

Proof. By Proposition B.1, $T_{\hat{P}}$ maps $\{F \in \mathbb{R}^{\mathcal{X} \times m} : F_m(x) = 0 \text{ for all } x \in \mathcal{X}\}$ to itself, and is a contraction on this subspace with respect to ℓ_2 , with contraction factor $\sqrt{\gamma}$. It therefore follows that $I - T_{\hat{P}}$ maps this subspace to itself, and is invertible on this subspace. Since $\sum_{k \geq 0} T_{\hat{P}}^k$ also maps this subspace to itself, it follows that on this subspace, we have $(I - T_{\hat{P}})^{-1} = \sum_{k \geq 0} T_{\hat{P}}^k$, as required. \square

Now, $(T_{\hat{P}} - T_P)F^* \in \{F \in \mathbb{R}^{\mathcal{X} \times m} : F_m(x) = 0 \text{ for all } x \in \mathcal{X}\}$, and hence from Equation (21) and Lemma E.1, it follows that

$$\hat{F} - F^* = \sum_{k \geq 0} T_{\hat{P}}^k (T_{\hat{P}} - T_P)F^*. \tag{22}$$

The result is that we have expressed the difference in CDFs in terms of local errors $(T_{\hat{P}} - T_P)F^*$, which are then propagated via the operator $\sum_{k \geq 0} T_{\hat{P}}^k$.

E.4. Bernstein concentration bounds

The next step in the proof is to establish a concentration bound for the local errors $(T_{\hat{P}} - T_P)F^*$.

One potential approach is to use a concentration inequality for each individual coordinate of $(T_{\hat{P}} - T_P)F^*$, indexed by (x, i) . Azar et al. (2013) note that in the mean-return case, using a Hoeffding-style bound is insufficient to obtain optimal dependence of the sample complexity on $(1 - \gamma)^{-1}$, and Zhang et al. (2023) also note this in their (non-categorical) distributional analysis. Using a Bernstein concentration inequality on each coordinate and then using a union bound can be made to work, although this then incurs a $\log(m)$ factor in the sample complexity. If such a dependence on m were tight, this would suggest that the sample complexity depends on m (albeit only logarithmically), and hence there would be a trade-off between picking m sufficiently large so as to obtain a low representation approximation error, as in Section E.2, and taking m low so as to not unduly increase the sample complexity. However, such a dependence on m can be avoided by working with concentration inequalities at the level of CDFs themselves. The Dvoretzky-Kiefer-Wolfowitz (DKW) inequality (Dvoretzky et al., 1956; Massart, 1990) behaves analogously to Hoeffding’s bound, and is insufficient for obtaining a sample complexity bound with optimal $(1 - \gamma)^{-1}$ dependence. Instead, we make use of a Hilbert space Bernstein-style inequality (Yurinsky, 2006; Chatalic et al., 2022), by interpreting the Cramér distance ℓ_2 as a maximum mean discrepancy (Gretton et al., 2012), which measures distances between distributions via embeddings in a (reproducing kernel) Hilbert space, allowing the Bernstein result to be applied.

First, we precisely describe the connection between Cramér distance and Hilbert space. Székely (2003) shows that for any distributions $\nu, \nu' \in \mathcal{P}([0, (1 - \gamma)^{-1}])$, we have

$$\ell_2^2(\nu, \nu') = \mathbb{E}_{X \sim \nu, Y \sim \nu'} [|X - Y|] - \frac{1}{2} \mathbb{E}_{X, X' \sim \nu} [|X - X'|] - \frac{1}{2} \mathbb{E}_{Y, Y' \sim \nu'} [|Y - Y'|]. \quad (23)$$

Sejdicinovic et al. (2013) show that there exists an affine embedding $\phi : \mathcal{P}([0, (1 - \gamma)^{-1}]) \rightarrow \mathcal{H}$ of distributions into a Hilbert space \mathcal{H} , such that the right-hand side of the equation can also be written as the squared norm $\|\phi(\nu) - \phi(\nu')\|_{\mathcal{H}}^2$; in other words, they show that the Cramér distance is equal to a squared maximum mean discrepancy (Gretton et al., 2012). We can then appeal to the following Bernstein-style inequality for Hilbert-space-valued random variables, which is due to Chatalic et al. (2022), and based largely on Yurinsky (2006, Theorem 3.3.4). We state the result here in the usual Bernstein style of assuming almost-sure boundedness of the the random variables concerned, while Chatalic et al. (2022) use the more general formulation of assuming particular bounds on all moments.

Lemma E.2. (Chatalic et al., 2022, Lemma E.3) *Let Z_1, \dots, Z_N be i.i.d. mean-zero random variables taking values in a Hilbert space $(\mathcal{H}, \|\cdot\|_{\mathcal{H}})$ such that $\|Z_1\|_{\mathcal{H}} \leq M$ almost surely. Then for any $\delta \in (0, 1)$, we have*

$$\left\| \frac{1}{N} \sum_{i=1}^N Z_i \right\|_{\mathcal{H}} \leq \frac{2M \log(2/\delta)}{N} + \sqrt{\frac{2\mathbb{E}[\|Z_1\|_{\mathcal{H}}^2] \log(2/\delta)}{N}},$$

with probability at least $1 - \delta$.

To apply this result in our setting, first note that, using the notation introduced in Appendix B, we have

$$\begin{aligned} \left\| [(T_{\hat{P}} - T_P)F^*](x) \right\|_{\ell_2} &= \ell_2((T_{\hat{P}}F^*)(x), F^*(x)) \\ &= \|\phi((T_{\hat{P}}F^*)(x)) - \phi(F^*(x))\|_{\mathcal{H}} \\ &\stackrel{(a)}{=} \left\| \phi \left(\frac{1}{N} \sum_{i=1}^N F^*(X_i^x) B_x^\top \right) - \phi(F^*(x)) \right\|_{\mathcal{H}} \\ &\stackrel{(b)}{=} \left\| \frac{1}{N} \sum_{i=1}^N \left(\phi(F^*(X_i^x) B_x^\top) - \phi(F^*(x)) \right) \right\|_{\mathcal{H}}, \end{aligned}$$

where (a) follows from the expressions for $T_{\hat{P}}$ described in Appendix B, and (b) follows from the affineness of the embedding ϕ . Here again, we make use of a slight abuse of notation by writing $\phi(F^*(x))$ for the embedding of the distribution supported on $\{z_1, \dots, z_m\}$, with CDF values $F^*(x)$, and similarly for embeddings of other CDF vectors.

We can now apply the result above, noting that

$$\|\phi(F^*(X_i^x)B_x^\top) - \phi(F^*(x))\|_{\mathcal{H}} = \ell_2(F^*(X_i^x)B_x^\top, F^*(x)) \leq (1 - \gamma)^{-1/2}$$

almost surely, and

$$\mathbb{E}\left[\|\phi(F^*(X_i^x)B_x^\top) - \phi(F^*(x))\|_{\mathcal{H}}^2\right] = \mathbb{E}\left[\ell_2^2(F^*(X_i^x)B_x^\top, F^*(x))\right] = \sigma(x),$$

where we write σ as shorthand for the local squared-Cramér variation at P , introduced in Definition 5.5 with the notation σ_P . Hence, from Lemma E.2 and a union bound over the state space \mathcal{X} , we obtain that with probability $1 - \delta/2$, we have for all $x \in \mathcal{X}$ that

$$\left\|[(T_{\hat{P}} - T_P)F^*](x)\right\|_{\ell_2} \leq C_{B1} \frac{\sqrt{\sigma(x)}}{\sqrt{N}} + C_{B2} \frac{1}{(1 - \gamma)^{1/2}N}, \quad (24)$$

where

$$C_{B1} = \sqrt{2 \log(4|\mathcal{X}|/\delta)}, \quad \text{and } C_{B2} = 2 \log(4|\mathcal{X}|/\delta).$$

E.5. From population to empirical squared-Cramér variation

Next, we show that the population local squared-Cramér variation in Equation (24) can be replaced with the corresponding *empirical* quantity; that is, the local-squared Cramér variation at \hat{P} , $\sigma_{\hat{P}}$, incurring some additional terms in the bound. We start by calculating as follows:

$$\begin{aligned} \sigma(x) &= \mathbb{E}\left[\|(\hat{T}_P F^*)(x) - (T_P F^*)(x)\|_{\ell_2}^2\right] \\ &= \mathbb{E}\left[\|F^*(X')B_x^\top\|_{\ell_2}^2\right] - \|P_x F^* B_x^\top\|_{\ell_2}^2 \\ &= P_x \|F^* B_x^\top\|_{\ell_2}^2 - \|P_x F^* B_x^\top\|_{\ell_2}^2, \end{aligned}$$

where above we use the notation $\|F^* B_x^\top\|_{\ell_2}^2 \in \mathbb{R}^{\mathcal{X}}$ for the vector indexed by state, so that the element corresponding to state $y \in \mathcal{X}$ is $\|F^*(y)B_x^\top\|_{\ell_2}^2$. To relate this quantity to $\hat{\sigma}(x)$, we add and subtract a term, motivated by the derivation applied to standard return variance by Azar et al. (2013, Lemma 5), and rearrange as follows:

$$\begin{aligned} &\sigma(x) \\ &= P_x \|F^* B_x^\top\|_{\ell_2}^2 - \|P_x F^* B_x^\top\|_{\ell_2}^2 \\ &= P_x \|F^* B_x^\top\|_{\ell_2}^2 - \|P_x F^* B_x^\top\|_{\ell_2}^2 - \left(\hat{P}_x \|F^* B_x^\top\|_{\ell_2}^2 - \|\hat{P}_x F^* B_x^\top\|_{\ell_2}^2\right) + \left(\hat{P}_x \|F^* B_x^\top\|_{\ell_2}^2 - \|\hat{P}_x F^* B_x^\top\|_{\ell_2}^2\right) \\ &= (P_x - \hat{P}_x) \|F^* B_x^\top\|_{\ell_2}^2 + \left(\|\hat{P}_x F^* B_x^\top\|_{\ell_2}^2 - \|P_x F^* B_x^\top\|_{\ell_2}^2\right) + \mathbb{E}\left[\|(\hat{T}_{\hat{P}} F^*)(x) - (T_{\hat{P}} F^*)(x)\|_{\ell_2}^2 \middle| \hat{P}\right] \\ &= (P_x - \hat{P}_x) \|F^* B_x^\top\|_{\ell_2}^2 + \langle \hat{P}_x F^* B_x^\top - P_x F^* B_x^\top, \hat{P}_x F^* B_x^\top + P_x F^* B_x^\top \rangle_{\ell_2} + \mathbb{E}\left[\|(\hat{T}_{\hat{P}} F^*)(x) - (T_{\hat{P}} F^*)(x)\|_{\ell_2}^2 \middle| \hat{P}\right] \\ &= (P_x - \hat{P}_x) \|F^* B_x^\top\|_{\ell_2}^2 + \langle (\hat{P}_x - P_x) F^* B_x^\top, \hat{P}_x F^* B_x^\top + P_x F^* B_x^\top \rangle_{\ell_2} + \mathbb{E}\left[\|(\hat{T}_{\hat{P}} F^*)(x) - (T_{\hat{P}} F^*)(x)\|_{\ell_2}^2 \middle| \hat{P}\right], \quad (25) \end{aligned}$$

where $\langle \cdot, \cdot \rangle_{\ell_2}$ is the inner product on \mathbb{R}^m corresponding to $\|\cdot\|_{\ell_2}$, defined by

$$\langle F, F' \rangle_{\ell_2} = \frac{1}{m(1 - \gamma)} \sum_{i=1}^m F_i F'_i.$$

Focusing on the final term on the right-hand side of Equation (25), we have

$$\begin{aligned}
 & \mathbb{E} \left[\left\| (\hat{T}_{\hat{P}} F^*) (x) - (T_{\hat{P}} F^*) (x) \right\|_{\ell_2}^2 \mid \hat{P} \right] \\
 = & \mathbb{E} \left[\left\| (\hat{T}_{\hat{P}} F^*) (x) - (\hat{T}_{\hat{P}} \hat{F}) (x) + (\hat{T}_{\hat{P}} \hat{F}) (x) - (T_{\hat{P}} F^*) (x) + (T_{\hat{P}} \hat{F}) (x) - (T_{\hat{P}} \hat{F}) (x) \right\|_{\ell_2}^2 \mid \hat{P} \right] \\
 = & \mathbb{E} \left[\left\| (\hat{T}_{\hat{P}} F^* - \hat{T}_{\hat{P}} \hat{F}) (x) - (T_{\hat{P}} F^* - T_{\hat{P}} \hat{F}) (x) + (\hat{T}_{\hat{P}} \hat{F}) (x) - (T_{\hat{P}} \hat{F}) (x) \right\|_{\ell_2}^2 \mid \hat{P} \right] \\
 = & \mathbb{E} \left[\left\| (\hat{T}_{\hat{P}} F^* - \hat{T}_{\hat{P}} \hat{F}) (x) - (T_{\hat{P}} F^* - T_{\hat{P}} \hat{F}) (x) \right\|_{\ell_2}^2 + 2 \langle (\hat{T}_{\hat{P}} F^* - \hat{T}_{\hat{P}} \hat{F}) (x) - (T_{\hat{P}} F^* - T_{\hat{P}} \hat{F}) (x), (\hat{T}_{\hat{P}} \hat{F} - T_{\hat{P}} \hat{F}) (x) \rangle_{\ell_2} \right. \\
 & \quad \left. + \left\| (\hat{T}_{\hat{P}} \hat{F}) (x) - (T_{\hat{P}} \hat{F}) (x) \right\|_{\ell_2}^2 \mid \hat{P} \right] \\
 \stackrel{(a)}{\leq} & \left(\mathbb{E} \left[\left\| (\hat{T}_{\hat{P}} F^* - \hat{T}_{\hat{P}} \hat{F}) (x) - (T_{\hat{P}} F^* - T_{\hat{P}} \hat{F}) (x) \right\|_{\ell_2}^2 \mid \hat{P} \right]^{1/2} + \mathbb{E} \left[\left\| (\hat{T}_{\hat{P}} \hat{F}) (x) - (T_{\hat{P}} \hat{F}) (x) \right\|_{\ell_2}^2 \mid \hat{P} \right]^{1/2} \right)^2 \\
 = & \left(\mathbb{E} \left[\left\| (\hat{T}_{\hat{P}} F^* - \hat{T}_{\hat{P}} \hat{F}) (x) - (T_{\hat{P}} F^* - T_{\hat{P}} \hat{F}) (x) \right\|_{\ell_2}^2 \mid \hat{P} \right]^{1/2} + \sqrt{\hat{\sigma}(x)} \right)^2.
 \end{aligned}$$

where (a) follows from the Cauchy-Schwarz inequality, and we write $\hat{\sigma}$ as a shorthand for $\sigma_{\hat{P}}$. Finally, we note that

$$\begin{aligned}
 \mathbb{E} \left[\left\| (\hat{T}_{\hat{P}} F^* - \hat{T}_{\hat{P}} \hat{F}) (x) - (T_{\hat{P}} F^* - T_{\hat{P}} \hat{F}) (x) \right\|_{\ell_2}^2 \mid \hat{P} \right] & \leq \mathbb{E} \left[\left\| (\hat{T}_{\hat{P}} F^* - \hat{T}_{\hat{P}} \hat{F}) (x) \right\|_{\ell_2}^2 \mid \hat{P} \right] \\
 & \stackrel{(a)}{\leq} \gamma \mathbb{E}_{X' \sim \hat{P}_x} \left[\left\| F^*(X') - \hat{F}(X') \right\|_{\ell_2}^2 \mid \hat{P} \right] \\
 & \leq \gamma \|F^* - \hat{F}\|_{\ell_2, \infty}^2,
 \end{aligned}$$

with (a) following from contractivity of B_x in $\|\cdot\|_{\ell_2}$, as established in Proposition B.2. Bringing these bounds together with Equation (25), we have

$$\sigma(x) \leq (P_x - \hat{P}_x) \|F^* B_x^\top\|_{\ell_2}^2 + \langle (\hat{P}_x - P_x) F^* B_x^\top, \hat{P}_x F^* B_x^\top + P_x F^* B_x^\top \rangle_{\ell_2} + \left(\gamma \|F^* - \hat{F}\|_{\ell_2, \infty} + \sqrt{\hat{\sigma}(x)} \right)^2. \quad (26)$$

We now apply concentration bounds to each of the first two terms on the right-hand side of Equation (26).

Lemma E.3. *With probability at least $1 - \delta/2$, we have for all $x \in \mathcal{X}$,*

$$\left| P_x \|F^* B_x^\top\|_{\ell_2}^2 - \hat{P}_x \|F^* B_x^\top\|_{\ell_2}^2 \right| \leq C_H \frac{1}{(1 - \gamma) \sqrt{N}},$$

where

$$C_H = \sqrt{\frac{\log(4|\mathcal{X}|/\delta)}{2}}.$$

Proof. The expression $P_x \|F^* B_x^\top\|_{\ell_2}^2 - \hat{P}_x \|F^* B_x^\top\|_{\ell_2}^2$ is equal to the negative of the average of N i.i.d. copies of the random variable $\|F^*(X') B_x^\top\|_{\ell_2}^2$, where $X' \sim P_x$, minus its expectation. Since $\|F^*(X') B_x^\top\|_{\ell_2}^2$ is bounded in $[0, (1 - \gamma)^{-1}]$, we apply Hoeffding's inequality (for a given $x \in \mathcal{X}$) to obtain

$$\left| P_x \|F^* B_x^\top\|_{\ell_2}^2 - \hat{P}_x \|F^* B_x^\top\|_{\ell_2}^2 \right| \leq \frac{1}{(1 - \gamma) \sqrt{N}} \sqrt{\frac{\log(4|\mathcal{X}|/\delta)}{2}},$$

with probability at least $1 - \delta/(2|\mathcal{X}|)$. Taking a union bound over $x \in \mathcal{X}$ then yields the statement. \square

For the second term, we may re-use the Bernstein concentration bound derived above to deduce the following.

Lemma E.4. *Suppose Equation (24) holds. Then we have, for all $x \in \mathcal{X}$,*

$$\left| \langle (\hat{P}_x - P_x) F^* B_x^\top, (\hat{P}_x + P_x) F^* B_x^\top \rangle_{\ell_2} \right| \leq 2C_{B1} \frac{1}{(1 - \gamma) \sqrt{N}} + 2C_{B2} \frac{1}{(1 - \gamma) N}.$$

Proof. First, by the Cauchy-Schwarz inequality, we have

$$\left| \langle (\hat{P}_x - P_x)F^*B_x^\top, (\hat{P}_x + P_x)F^*B_x^\top \rangle_{\ell_2} \right| \leq \|(\hat{P}_x - P_x)F^*B_x^\top\|_{\ell_2} \|(\hat{P}_x + P_x)F^*B_x^\top\|_{\ell_2}.$$

The first of the two factors in the product on the right-hand side is precisely the term bounded on the left-hand side of Equation (24). On the right-hand side, the vector inside the ℓ_2 -norm has components in $[0, 2]$, so the norm can be straightforwardly bounded by

$$\left[\frac{1}{m(1-\gamma)} \sum_{i=1}^m 2^2 \right]^{1/2} = \frac{2}{(1-\gamma)^{1/2}}.$$

Combining the inequalities for these two factors, and using the trivial bound $\sqrt{\sigma(x)} \leq (1-\gamma)^{-1/2}$, we obtain the stated result. \square

Combining all these bounds together in Equation (26), and taking a union bound, we conclude that with probability at least $1 - \delta/2$, for all $x \in \mathcal{X}$ we have

$$\sigma(x) \leq (2C_{B1} + C_H) \frac{1}{(1-\gamma)\sqrt{N}} + 2C_{B2} \frac{1}{(1-\gamma)N} + \left(\gamma \|F^* - \hat{F}\|_{\ell_2, \infty} + \sqrt{\hat{\sigma}(x)} \right)^2,$$

We now take square-roots of both sides, using the inequality $\sqrt{a+b} \leq \sqrt{a} + \sqrt{b}$ on the right-hand side to obtain

$$\sqrt{\sigma(x)} \leq \sqrt{\hat{\sigma}(x)} + \gamma \|F^* - \hat{F}\|_{\ell_2, \infty} + \sqrt{2C_{B1} + C_H} \frac{1}{(1-\gamma)^{1/2}N^{1/4}} + \sqrt{2C_{B2}} \frac{1}{(1-\gamma)^{1/2}N^{1/2}}.$$

Substituting this into Equation (24) and taking a union bound then yields that with probability at least $1 - \delta$, we have

$$\left\| [(T_{\hat{P}} - T_P)F^*](x) \right\|_{\ell_2} \leq C_{B1} \frac{1}{\sqrt{N}} \sqrt{\hat{\sigma}(x)} + C_{B1} \frac{1}{\sqrt{N}} \|F^* - \hat{F}\|_{\ell_2, \infty} + C' \frac{1}{(1-\gamma)^{1/2}N^{3/4}}, \quad (27)$$

where

$$C' = C_{B1}(\sqrt{2C_{B1} + C_H} + \sqrt{2C_{B2}}) + C_{B2},$$

so that our concentration inequality is expressed in terms of the empirical local squared-Cramér variation $\hat{\sigma}$.

E.6. Converting local bounds to global bounds

To convert the local concentration results obtained above into a bound on $\ell_2(\hat{F}(x), F^*(x))$, we first prove the following lemma.

Lemma E.5. *For $U \in \{F \in \mathbb{R}^{\mathcal{X} \times m} : F_m(x) = 0 \text{ for all } x \in \mathcal{X}\}$, and any $k \geq 1$, we have*

$$\|(T_{\hat{P}}^k U)(x)\|_{\ell_2} \leq \gamma^{k/2} \sum_{x' \in \mathcal{X}} \mathbb{P}_{\hat{P}}(X_k = x' \mid X_0 = x) \|U(x')\|_{\ell_2},$$

where $\mathbb{P}_{\hat{P}}$ denotes state transition probabilities for the MRP with transition matrix \hat{P} .

Proof. We proceed by induction. For the base case $k = 1$, we have, using the operator notation introduced in Appendix B,

$$\begin{aligned} \|(T_{\hat{P}} U)(x)\|_{\ell_2} &= \left\| \sum_{y \in \mathcal{X}} \hat{P}(y|x) \sum_{j=1}^{m-1} B_x U(y) \right\|_{\ell_2} \\ &\stackrel{(a)}{\leq} \sum_{y \in \mathcal{X}} \hat{P}(y|x) \left\| B_x U(y) \right\|_{\ell_2} \\ &\stackrel{(b)}{\leq} \sum_{y \in \mathcal{X}} \hat{P}(y|x) \gamma^{1/2} \left\| U(y) \right\|_{\ell_2}, \end{aligned}$$

as required. where (a) follows from the triangle inequality, and (b) follows from contractivity of B_x in $\|\cdot\|_{\ell_2}$, as established by Proposition B.2.

For the inductive step, we suppose that the result holds for some $l \in \mathbb{N}$. Now, letting $k = l + 1$, we have

$$\begin{aligned}
 \|(T_{\hat{P}}^{l+1}U)(x)\|_{\ell_2} &= \|(T_{\hat{P}}T_{\hat{P}}^lU)(x)\|_{\ell_2} \\
 &= \left\| \sum_{y \in \mathcal{X}} \hat{P}(y|x)B_x(T_{\hat{P}}^lU)(y) \right\|_{\ell_2} \\
 &\leq \sum_{y \in \mathcal{X}} \hat{P}(y|x) \left\| B_x(T_{\hat{P}}^lU)(y) \right\|_{\ell_2} \\
 &\leq \sum_{y \in \mathcal{X}} \hat{P}(y|x)\gamma^{1/2} \left\| (T_{\hat{P}}^lU)(y) \right\|_{\ell_2} \\
 &\stackrel{(a)}{\leq} \sum_{y \in \mathcal{X}} \hat{P}(y|x)\gamma^{1/2}\gamma^{l/2} \sum_{x' \in \mathcal{X}} \mathbb{P}_{\hat{P}}(X_l = x' | X_0 = y) \|U(x')\|_{\ell_2} \\
 &= \gamma^{(l+1)/2} \sum_{x' \in \mathcal{X}} \left[\sum_{y \in \mathcal{X}} \mathbb{P}_{\hat{P}}(X_l = x' | X_0 = y) \hat{P}(y|x) \right] \|U(x')\|_{\ell_2} \\
 &= \gamma^{(l+1)/2} \sum_{x' \in \mathcal{X}} \mathbb{P}_{\hat{P}}(X_{l+1} = x' | X_0 = x) \|U(x')\|_{\ell_2},
 \end{aligned}$$

as required, where (a) follows by the inductive hypothesis. \square

We therefore have, with probability at least $1 - \delta$:

$$\begin{aligned}
 &\ell_2(\hat{F}(x), F^*(x)) \tag{28} \\
 &= \|\hat{F}(x) - F^*(x)\|_{\ell_2} \\
 &\stackrel{(a)}{=} \left\| \left[\sum_{k \geq 0} T_{\hat{P}}^k(T_{\hat{P}} - T_P)F^* \right](x) \right\|_{\ell_2} \\
 &\stackrel{(b)}{\leq} \sum_{k \geq 0} \left\| \left[T_{\hat{P}}^k(T_{\hat{P}} - T_P)F^* \right](x) \right\|_{\ell_2} \\
 &\stackrel{(c)}{\leq} \sum_{k \geq 0} \sum_{x' \in \mathcal{X}} \mathbb{P}_{\hat{P}}(X_k = x' | X_0 = x) \gamma^{k/2} \left\| \left[(T_{\hat{P}} - T_P)F^* \right](x') \right\|_{\ell_2} \\
 &\stackrel{(d)}{\leq} \sum_{k \geq 0} \sum_{x' \in \mathcal{X}} \mathbb{P}_{\hat{P}}(X_k = x' | X_0 = x) \gamma^{k/2} \left[C_{B1} \frac{1}{\sqrt{N}} \sqrt{\hat{\sigma}(x')} + C_{B1} \frac{1}{\sqrt{N}} \|F^* - \hat{F}\|_{\ell_2, \infty} + C' \frac{1}{(1 - \gamma)^{1/2} N^{3/4}} \right] \\
 &\stackrel{(e)}{\leq} \frac{C_{B1}}{\sqrt{N}} \|(I - \sqrt{\gamma}\hat{P})^{-1}\sqrt{\hat{\sigma}}\|_{\infty} + \frac{C_{B1}}{(1 - \sqrt{\gamma})\sqrt{N}} \|F^* - \hat{F}\|_{\ell_2, \infty} + \frac{C'}{(1 - \sqrt{\gamma})(1 - \gamma)^{1/2} N^{3/4}} \\
 &\stackrel{(f)}{\leq} \frac{C_{B1}}{\sqrt{N}} \|(I - \sqrt{\gamma}\hat{P})^{-1}\sqrt{\hat{\sigma}}\|_{\infty} + \frac{2C_{B1}}{(1 - \gamma)\sqrt{N}} \|F^* - \hat{F}\|_{\ell_2, \infty} + \frac{2C'}{(1 - \gamma)^{3/2} N^{3/4}}. \tag{29}
 \end{aligned}$$

Here, (a) follows from Equation (22), (b) follows from the triangle inequality, and (c) follows from Lemma E.5. The step (d) is the one step in the derivation that does not hold with probability 1, but rather with probability $1 - \delta$, and follows from the Bernstein-style bounds in Equation (27), (e) follows from algebraic manipulation using the identity $\sum_{k \geq 0} (\gamma^{1/2}\hat{P})^k = (I - \sqrt{\gamma}\hat{P})^{-1}$, as \hat{P} is a stochastic matrix, and bounding the elements of $(I - \sqrt{\gamma}\hat{P})^{-1}\sqrt{\hat{\sigma}}$ by the L^∞ norm of the vector, and (f) follows from the inequality $(1 - \sqrt{\gamma})^{-1} \leq 2(1 - \gamma)^{-1}$ for $\gamma \in [0, 1)$.

Focusing now on the coefficient $\|(I - \sqrt{\gamma}\hat{P})^{-1}\sqrt{\hat{\sigma}}\|_{\infty}$, we note that similar to the analysis of Agarwal et al. (2020, Lemma 4) in the mean-return case, we can write

$$(I - \sqrt{\gamma}\hat{P})^{-1}\sqrt{\hat{\sigma}} = (1 - \sqrt{\gamma})^{-1}(1 - \sqrt{\gamma})(I - \sqrt{\gamma}\hat{P})^{-1}\sqrt{\hat{\sigma}},$$

so that each row of

$$(1 - \sqrt{\gamma})(I - \sqrt{\gamma}\hat{P})^{-1}$$

forms a probability distribution, and so we may apply Jensen's inequality with the map $z \mapsto \sqrt{z}$, to obtain

$$(I - \sqrt{\gamma}\hat{P})^{-1}\sqrt{\hat{\sigma}} \leq (1 - \sqrt{\gamma})^{-1}\sqrt{(1 - \sqrt{\gamma})(I - \sqrt{\gamma}\hat{P})^{-1}\hat{\sigma}} = (1 - \sqrt{\gamma})^{-1/2}\sqrt{(I - \sqrt{\gamma}\hat{P})^{-1}\hat{\sigma}}, \quad (30)$$

where the inequality above holds coordinate-wise. We thus obtain the inequality

$$\|F^* - \hat{F}\|_{\ell_2, \infty} \leq \frac{2C_{B1}}{(1 - \gamma)^{1/2}\sqrt{N}} \sqrt{\|(I - \sqrt{\gamma}\hat{P})^{-1}\sqrt{\hat{\sigma}}\|_{\infty}} + \frac{2C_{B1}}{(1 - \gamma)\sqrt{N}} \|F^* - \hat{F}\|_{\ell_2, \infty} + \frac{2C'}{(1 - \gamma)^{3/2}N^{3/4}}.$$

Note that the term $\|F^* - \hat{F}\|_{\ell_2, \infty}$ appears on both sides of the inequality above. By taking $N \geq 16C_{B1}^2(1 - \gamma)^{-2}$, we ensure that the coefficient in front of $\|F^* - \hat{F}\|_{\ell_2, \infty}$ on the right-hand side is made smaller than $1/2$, similar to the approach taken in the proof of instance-dependent sample complexity bounds for mean-return estimation by Pananjady & Wainwright (2020, Theorem 1(a)). Under this assumption, rearrangement yields

$$\|F^* - \hat{F}\|_{\ell_2, \infty} \leq \frac{4C_{B1}}{(1 - \gamma)^{1/2}\sqrt{N}} \sqrt{\|(I - \sqrt{\gamma}\hat{P})^{-1}\sqrt{\hat{\sigma}}\|_{\infty}} + \frac{4C'}{(1 - \gamma)^{3/2}N^{3/4}} \quad (31)$$

as described in Section 5.

E.7. The stochastic categorical CDF Bellman equation

We now aim to use our developments regarding the stochastic categorical CDF Bellman equation (see Section 5.2) to bound the quantity appearing within the square root. To be able to use the bound obtained in Corollary 5.12, we first replace the factor $\sqrt{\gamma}$ inside the square-root on the right-hand side of Equation (30) with γ , using the bound $(I - \sqrt{\gamma}P)^{-1} \leq 2(I - \gamma P)^{-1}$, shown by Agarwal et al. (2020, Lemma 4). This, together with Corollary 5.12, yields

$$\sqrt{(I - \sqrt{\gamma}\hat{P})^{-1}\hat{\sigma}} \leq \sqrt{2}\sqrt{(I - \gamma\hat{P})^{-1}\hat{\sigma}} \leq \sqrt{2}\sqrt{\frac{2}{1 - \gamma}}\mathbf{1} = \frac{2}{(1 - \gamma)^{1/2}}\mathbf{1}.$$

Thus, returning to Equation (31) and substituting this bound in, we obtain (again, with probability at least $1 - \delta$, for all $x \in \mathcal{X}$):

$$\ell_2(\hat{F}(x), F^*(x)) \leq \frac{8C_{B1}}{(1 - \gamma)\sqrt{N}} + \frac{4C'}{(1 - \gamma)^{3/2}N^{3/4}} \quad (32)$$

E.8. Final steps of the proof of Theorem 5.3

We now let $N \geq c_0\varepsilon^{-2}(1 - \gamma)^{-2}$, with c_0 any positive number satisfying

$$c_0 \geq 2^{10}C_{B1}^2 \text{ and } c_0 > 16^{4/3}(C')^{4/3}. \quad (33)$$

Note that the first of these conditions implies the earlier assumption $N \geq 16C_{B1}^2(1 - \gamma)^{-2}$ made in order to arrive at Equation (31). We then conclude from Equation (32) that (with probability at least $1 - \delta$, for all $x \in \mathcal{X}$):

$$\begin{aligned} \ell_2(\hat{F}(x), F^*(x)) &\leq \frac{8C_{B1}}{\sqrt{c_0}}\varepsilon + \frac{4C'}{c_0^{3/4}}\varepsilon^{3/2} \\ &\leq \frac{8C_{B1}}{\sqrt{c_0}}\varepsilon + \frac{4C'}{c_0^{3/4}}\varepsilon \\ &\leq \varepsilon/2, \end{aligned}$$

with the final inequality following due to the assumption on c_0 making both coefficients of ε bounded by $1/4$. This concludes the proof of Theorem 5.3.

To derive a concrete sample complexity bound, including logarithmic terms, we may bound the terms in Equation (33) as follows; we emphasise that we do not aim to be as tight as possible in the following analysis, but merely to provide an concrete, valid bound on c_0 . First, we have that the

$$\begin{aligned} 2^{10} C_{B1}^2 &= 2^{10} (\sqrt{2 \log(4|\mathcal{X}|/\delta)})^2 \\ &= 2^{11} \log(4|\mathcal{X}|/\delta). \end{aligned}$$

Next, we have (introducing the shorthand $L = \log(4|\mathcal{X}|/\delta)$):

$$\begin{aligned} 16^{4/3} (C')^{4/3} &\leq 2^6 \left(C_{B1} (\sqrt{2C_{B1}} + C_H + \sqrt{2C_{B2}}) + C_{B2} \right)^{4/3} \\ &= 2^6 (\sqrt{2L} (\sqrt{2\sqrt{2L}} + \sqrt{L/2} + \sqrt{4L}) + 2L)^{4/3} \\ &\leq 2^6 (L\sqrt{2} (\sqrt{2\sqrt{2}} + \sqrt{1/2} + 2) + 2L)^{4/3} \\ &= 2^6 L^{4/3} (\sqrt{2} (\sqrt{2\sqrt{2}} + \sqrt{1/2} + 2) + 2)^{4/3} \\ &\leq 2^6 L^{4/3} 2^4 \\ &= 2^{10} L^{4/3}. \end{aligned}$$

We therefore conclude, for example, that taking $c_0 \geq 2^{11} \log(4|X|/\delta)^{4/3}$ is sufficient.

F. Further experimental results and details

In this section, we give full details for the experiment presented in the main paper, and additionally present extended results on several additional environments. All experiments were run using the Python 3 language (Van Rossum & Drake, 2009), and made use of NumPy (Harris et al., 2020), SciPy (Virtanen et al., 2020), Matplotlib (Hunter, 2007), and Seaborn (Waskom, 2021) libraries.

F.1. Environments

We report results on four MRPs defined as follows:

1. **Chain:** 10 states arranged in a chain $x_1 \leftrightarrow x_2 \leftrightarrow \dots \leftrightarrow x_{10}$. Each state transitions to its neighbours with equal probability. States 1 and 10 are terminal. Only state 10 has a reward of 1, and all other states have reward 0.
2. **Low random:** There are five states, and the transition probabilities from each state to all five states are drawn independently from a Dirichlet distribution with concentration parameter $(0.01, \dots, 0.01)$. The rewards for each state is drawn i.i.d. from the uniform distribution over $[0, 1]$. We draw these transition probability and rewards using the same random seed to yield the same MRP for all experiments.
3. **High random:** Same as the low random environment, but with transitions drawn from a Dirichlet distribution with concentration parameter $(10, \dots, 10)$.
4. **Two-state:** A 2-state MRP modified from Example 6.5 of Rowland et al. (2023). The transition matrix is

$$\begin{pmatrix} 0.6 & 0.4 \\ 0.8 & 0.2 \end{pmatrix}$$

where the (i, j) entry is the probability of transitioning from state i to state j . State 1 has reward 0, and state 2 has reward 1.

We chose this set of environments to include classic tabular settings such as the chain, two environments with very different levels of stochasticity (low and high random), as well as the two-state example from Rowland et al. (2023), which illustrates the nature of fixed-point approximation error incurred by QDP in environments with tight bootstrapping loops. We vary the

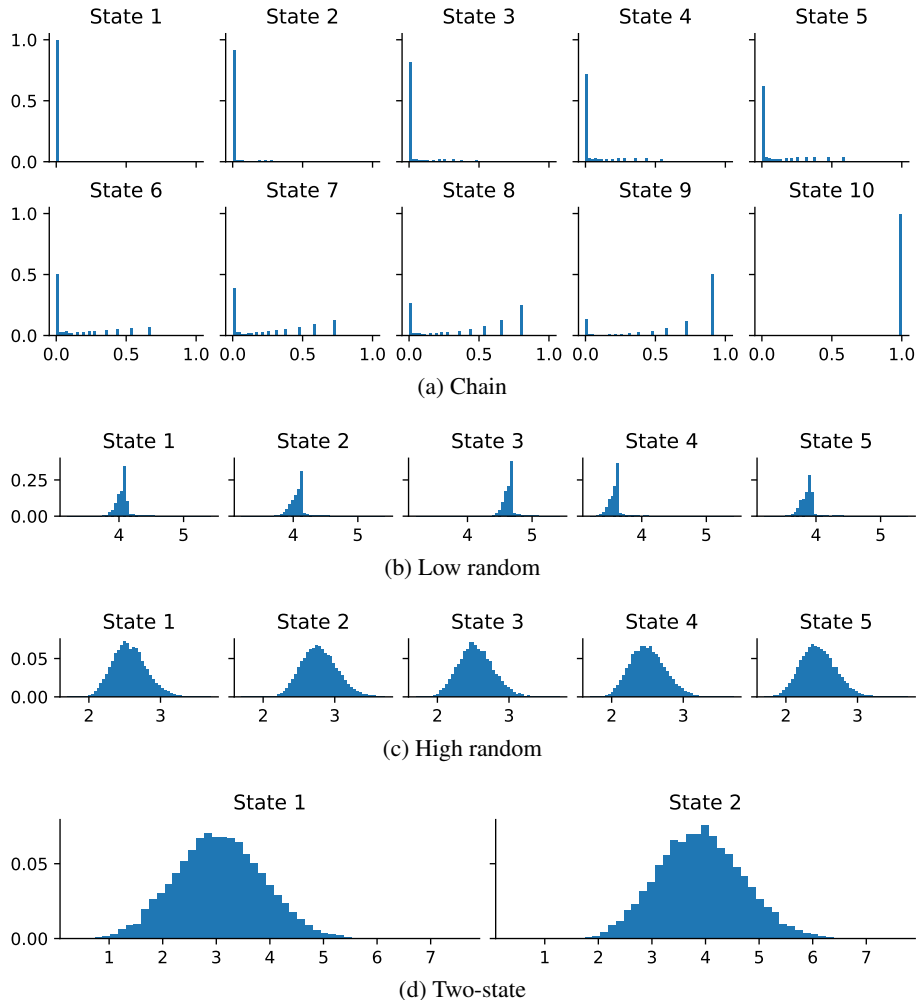


Figure 4. Monte Carlo approximations of return distributions in each of the four environments tested.

discount factor $\gamma \in \{0.8, 0.9, 0.95, 0.99\}$. For reference, we plot Monte Carlo approximations of return distributions for each environment in Figure 4, with $\gamma = 0.9$. The return samples are computed using the first-visit Monte Carlo algorithm. For each initial state, we run at least T transitions such that the maximum error after T transitions $\gamma^T r_{\max}/(1-\gamma) < \epsilon$, where $r_{\max} = 1$ and we set $\epsilon = 10^{-4}$. This is repeated 10^4 times for each state, giving at least 10^4 return samples per state.

F.2. Algorithms

As described in the main paper, we compare DCFP, QDP, and CDP algorithms. For DCFP and CDP, we make use of the sparse structure of the update matrix (see Equation (9)), and implement these algorithms using SciPy’s sparse matrix-vector multiplication and linear system solution methods (Virtanen et al., 2020). The mathematical details regarding the sparsity of the update matrix is described in Appendix F.3. For comparison, we also run implementations of DCFP and CDP that do not exploit this sparsity, and instead use standard dense NumPy implementations for matrix-vector multiplication and linear system solution methods; these are denoted by d-DCFP and d-CDP, respectively.

By default the categorical methods (all variants of DCFP and CDP) use the atom locations described in the main paper: $z_i = \frac{i-1}{m-1}(1-\gamma)^{-1}$ for $i = 1, \dots, m$. These atom locations are sufficient to establish the theoretical results in the main paper, though we note that in practice, particularly when true return distributions are localised within a small sub-interval of $[0, (1-\gamma)^{-1}]$, this setting can be overly conservative. However, in many cases, there are straightforward ways in which the choice of support can be improved, essentially by replacing the uniformly valid return range $[0, (1-\gamma)^{-1}]$ with an *a priori* known environment-specific reward range. As an example, if the known range of immediate rewards forms a sub-interval

$[r_{\min}, r_{\max}] \subseteq [0, 1]$, then the return must fall into the environment-specific reward range $[r_{\min}(1-\gamma)^{-1}, r_{\max}(1-\gamma)^{-1}]$, and improved atom locations $z_i = r_{\min}(1-\gamma)^{-1} + \frac{i-1}{m-1}(r_{\max}-r_{\min})(1-\gamma)^{-1}$ (for $i = 1, \dots, m$) can be used, whilst maintaining the guarantee that the support for the true return distributions lie within this interval. We thus additionally report results for versions of DCFP and CDP that use environment-specific atom locations, to investigate what practical improvements can be gained with such additional information. Specifically, for the high random and low random environments, we use the tighter bounds on support given by known r_{\min} and r_{\max} , as described above. In the chain environment, we consider using the advanced knowledge that only the transition into the terminal state is rewarding, yielding a sub-interval for possible returns of $[0, 1]$. In the two-state case, the range of possible returns is the full interval $[0, (1-\gamma)^{-1}]$, and so we do not investigate an environment-specific set of atoms in this case. However, it is clear from the Monte Carlo approximations to the return distributions in this environment in Figure 4 that these distributions do have the vast majority of their probability mass in a much smaller interval than the worst case interval $[0, (1-\gamma)^{-1}]$.

We ran all DP methods with 30,000 iterations. For all categorical DP methods, we verify that the Wasserstein distance between the last iterate to the Monte Carlo ground truth is almost identical to the Wasserstein distance between the categorical fixed-point to the ground truth.

E.3. Efficient implementation of CDP and DCFP

A straightforward implementation of CDP and DCFP is to vectorise F , treating it as a vector indexed by state-index pairs (x, i) , and correspondingly treat $T_{\hat{P}}$ as a matrix whose rows and columns are indexed similarly. Iterations of CDP can then be performed by simple matrix-vector multiplications with this representation of $T_{\hat{P}}$, and the solution of the linear system appearing in Equation (11) that forms the core of DCFP can be implemented with a call to a standard linear system solver, such as `numpy.linalg.solve` (Harris et al., 2020).

However, the operator $T_{\hat{P}}$ typically has some specific structure that can be exploited in implementations. In particular, we highlight here the sparse structure of $T_{\hat{P}}$, allowing for potential speed-ups in implementation by making use of sparse linear solvers, such as `scipy.sparse.linalg.spsolve` (Virtanen et al., 2020). Recall that, viewing $T_{\hat{P}}$ as a matrix (c.f. Equation (9)), the element corresponding to the (x, i) row and (y, j) column is given by

$$\hat{P}(y|x)(H_{i,j}^x - H_{i,j+1}^x). \quad (34)$$

In an MRP with sparse transition matrix P , the empirical estimate \hat{P} inherits this sparsity, inducing sparsity in $T_{\hat{P}}$. In addition, there is also sparsity induced by the atom index components of the row and column indices, as we now describe. Recall from Equation (8) that $H_{i,j}^x = \sum_{l \leq i} h_l(r(x) + \gamma z_j)$; see Figure 5 for an illustration the function $z \mapsto \sum_{l \leq i} h_l(z)$.

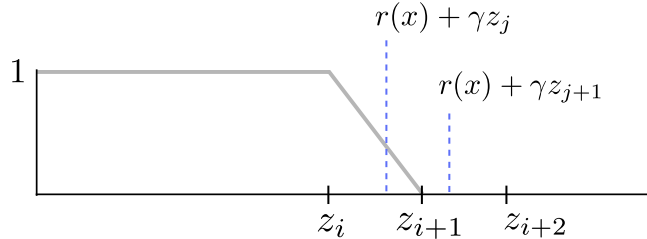


Figure 5. The function $z \mapsto \sum_{l \leq i} h_l(z)$ (grey), and a possible configuration for $r(x) + \gamma z_j, r(x) + \gamma z_{j+1}$ in the event of a non-zero $H_{i,j}^x - H_{i,j+1}^x$ term.

Now, suppose that for some $x \in \mathcal{X}$ and $1 \leq i, j \leq m-1$, $H_{i,j}^x - H_{i,j+1}^x$ is non-zero. This says that the function $z \mapsto \sum_{l \leq i} h_l(z)$ takes on different values at $r(x) + \gamma z_j$ and $r(x) + \gamma z_{j+1}$, and since the distance between these arguments is γ times the grid width $(1-\gamma)^{-1}m^{-1}$, it follows that at least one of these two arguments must lie in the interval $[z_i, z_{i+1}]$; see Figure 5.

From this observation, we deduce two forms of sparsity for the elements given in Equation (34). First, since one of $r(x) + \gamma z_j$ and $r(x) + \gamma z_{j+1}$ must lie in $[z_i, z_{i+1}]$, we deduce that neither of these points can lie in any interval $[z_{i'}, z_{i'+1}]$ with $i' < i-1$ or $i' > i+1$, and hence $H_{i',j}^x - H_{i',j+1}^x = 0$ for such i' . From this reasoning, it follows that ranging over i in Equation (34), there are at most 2 non-zero elements. For large m , this means that $T_{\hat{P}}$ is very sparse.

Similarly, we can deduce row sparsity by noting that at most $\lceil 2/\gamma \rceil$ indices j can have the property that $r(x) + \gamma z_j$ or

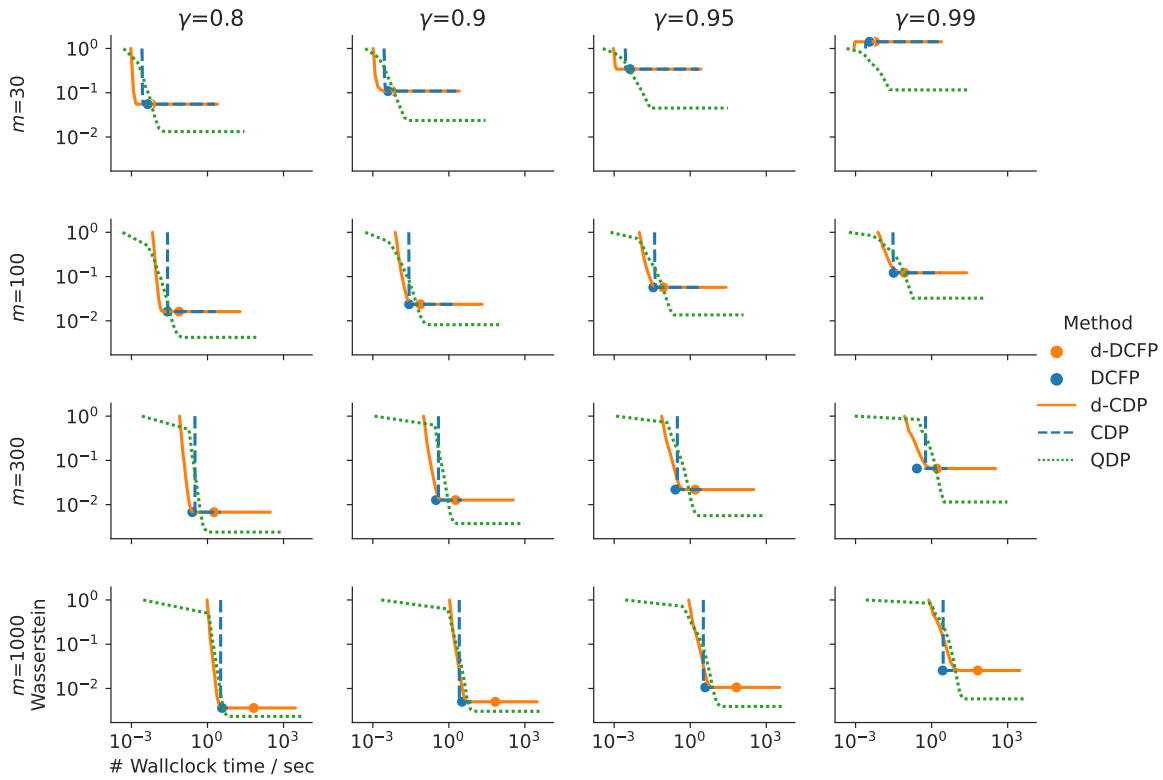
$r(x) + \gamma z_{j+1}$ can lie in $[z_i, z_{i+1}]$, and it is only for these indices j that we can have $H_{i,j}^x - H_{i,j+1}^x$ non-zero. So for $\gamma \approx 1$, this also implies sparsity of the elements in Equation (34) as we range over j .

F.4. Results

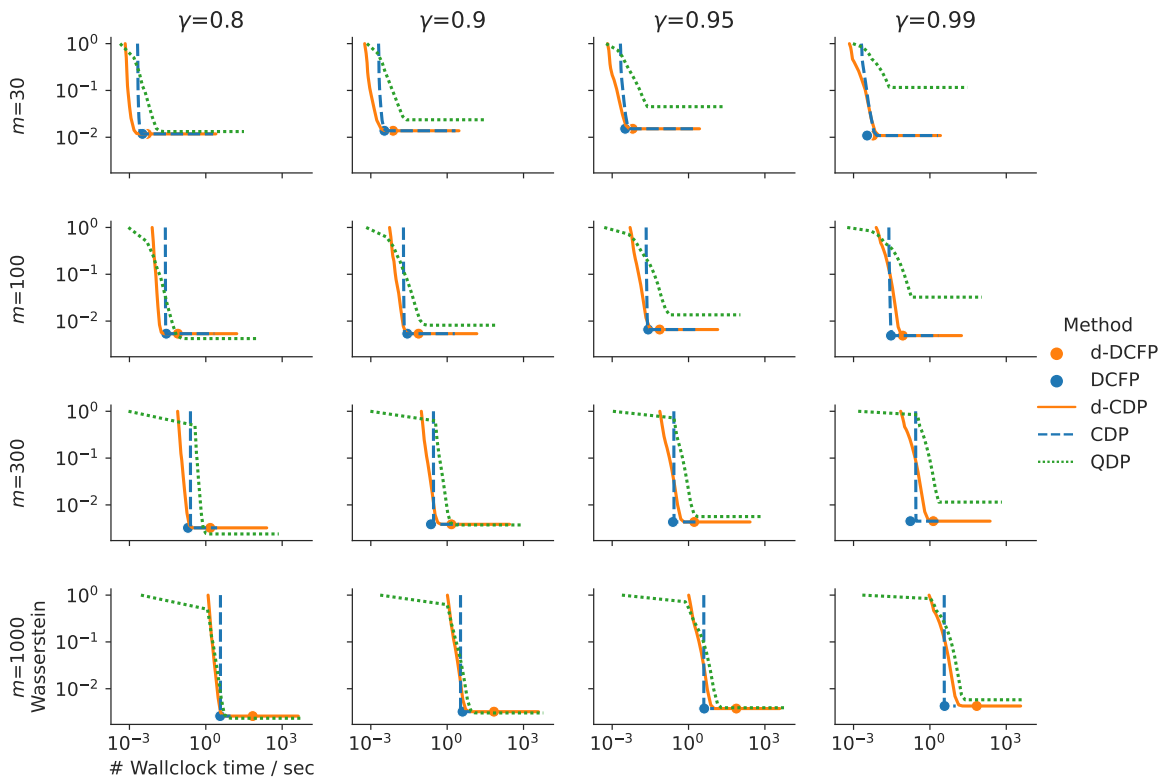
For each setting, we repeat the experiment 30 times with different sampled transitions. We display trade-off plots (supremum-Wasserstein-1 error and wallclock time) for each of the four environments described above, in Figures 6, 7, 8, and 9, for the cases of $m \in \{30, 100, 300, 1000\}$ atoms and using $N = 10^6$ sample transitions from each state to estimate transition matrix. These curves are obtained by averaging across the 30 repetitions. Some central themes emerge from the results.

In the case when the categorical methods use the environment-independent, standard atom locations $z_i = \frac{i-1}{m-1}(1-\gamma)^{-1}$ for $i = 1, \dots, m$, we find that for a given atom count m , QDP often achieves the lowest asymptotic Wasserstein-1 error. A notable exception is the two-state environment; Rowland et al. (2023) observed that such environments, in which there is a short, high-probability path from a state to itself, can cause high approximation error for QDP, which we believe is the cause of the inaccuracy observed here, particularly at high discounts. However, the categorical approaches often deliver better performance as judged by wallclock time. This is owing to the efficient implementations of the linear operator, and solution methods for the linear system, that are associated with these algorithms. By contrast, the QDP operator is non-linear, and requires a call to a sorting method. We tend to observe the greatest benefits of the sparse implementation for large atom counts, as expected, and also observe the greatest benefits of DCFP over the iterative CDP algorithm in settings with high discount factors. This is also to be expected, since the discount factor controls the rate of convergence of the DP algorithms. Note additionally that the use of environment-specific atom locations generally improves the results obtained with categorical approaches; the improvements in the chain environment are particularly strong, since the narrow return range allows for a denser packing of atom locations, by a factor of $(1-\gamma)^{-1}$, for a given atom count m .

We also compare how the supremum-Wasserstein distance changes while the number of samples used to estimate \hat{P} increases from 10^2 to 10^6 . Since the categorical methods all converge to the same fixed point, we only show the result of DCFP and QDP, using $m \in \{30, 100, 300, 1000\}$ atoms. Figure 10(a) shows that the distance decreases as the number of samples increase. One exception is the QDP with 30 atoms applied to high random at high γ , where $N = 100$ produced smallest distance on average. Figure 10(b) shows the results when the environment-specific return range is given. This substantially reduced the supremum-Wasserstein distance, especially when using a small number of atoms.

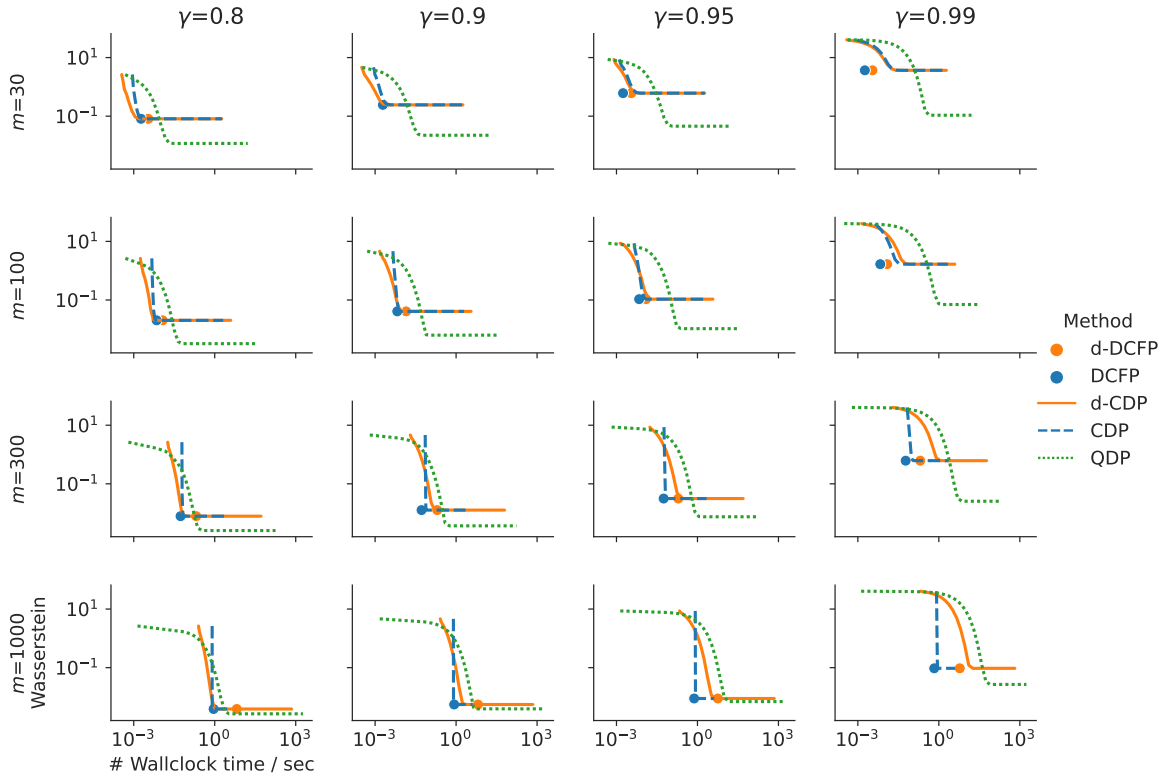


(a) Global return range

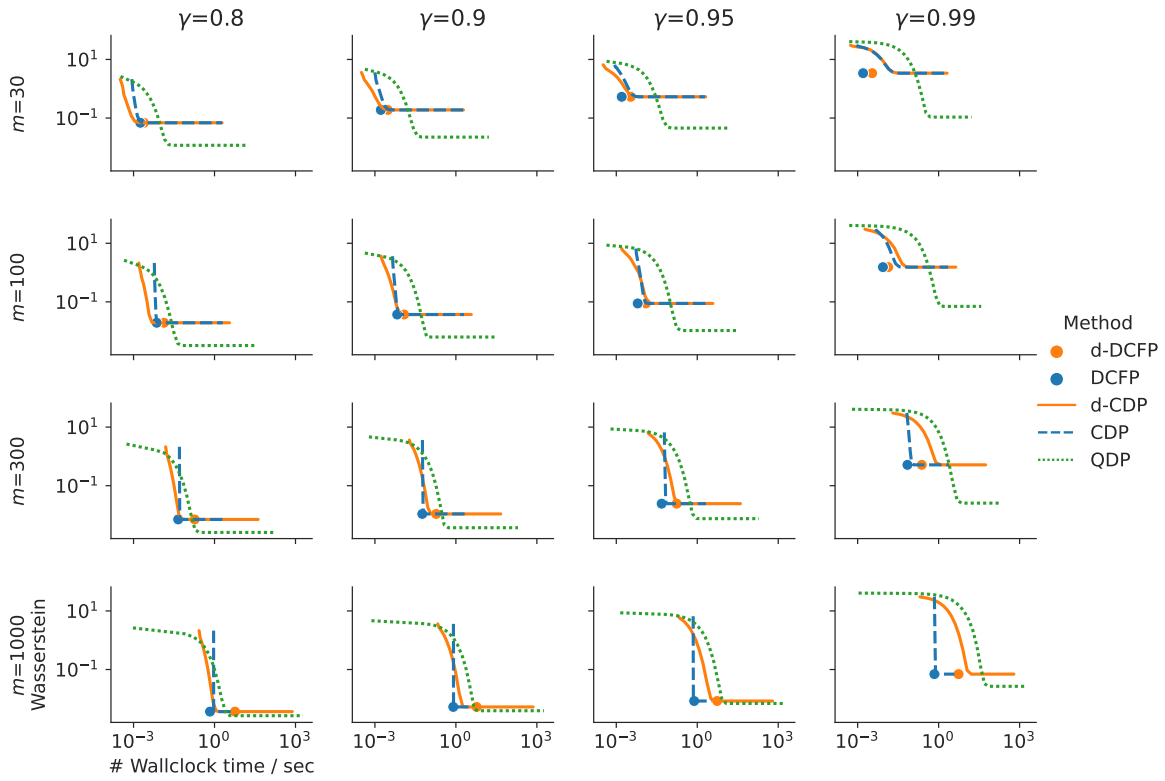


(b) Environment-specific return range

Figure 6. Distance vs. run time results for the chain environment, for \hat{P} estimated from $N = 10^6$ sample transitions.

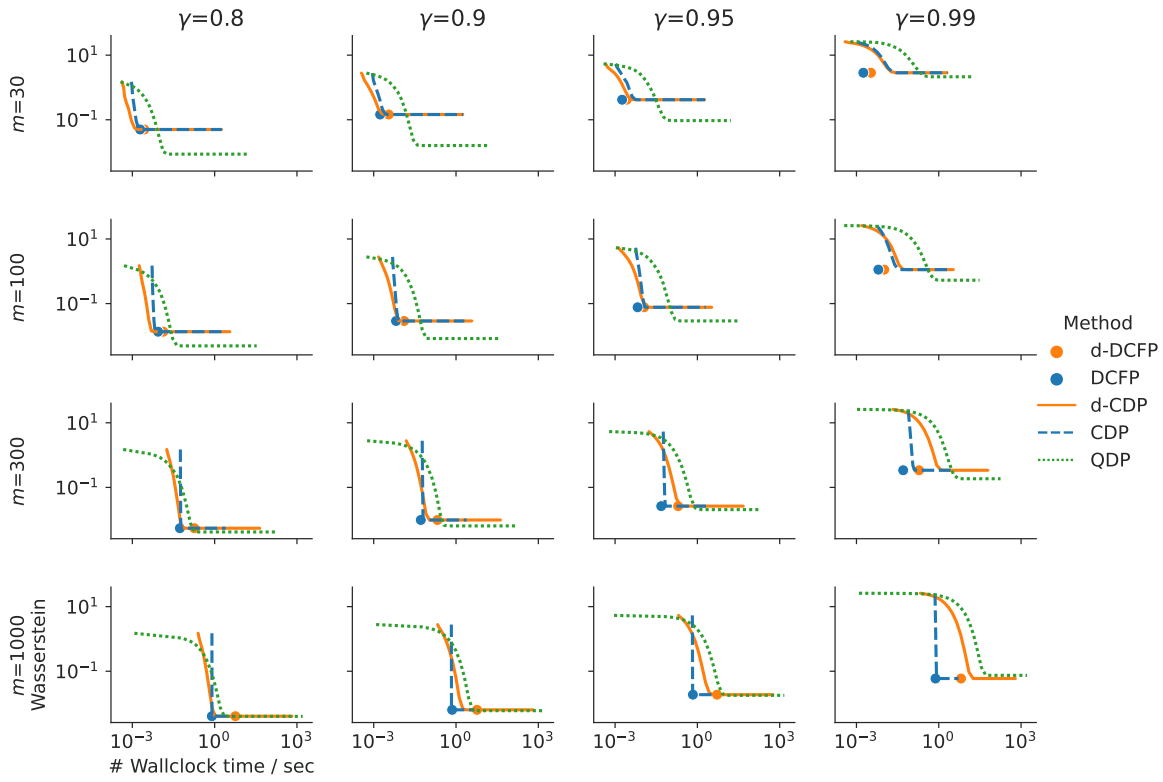


(a) Global return range

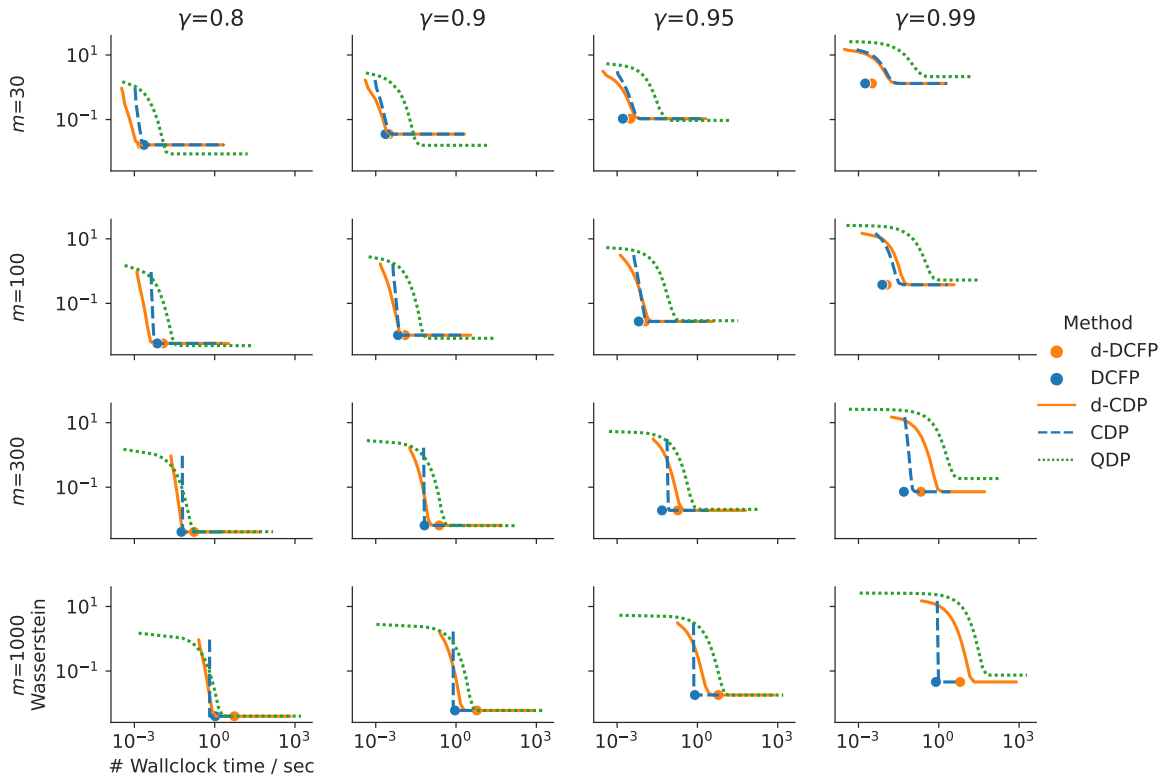


(b) Environment-specific return range

Figure 7. Distance vs. run time results for the low random environment, for \hat{P} estimated from $N = 10^6$ sample transitions.



(a) Global return range



(b) Environment-specific return range

Figure 8. Distance vs. run time results for the high random environment, for \hat{P} estimated from $N = 10^6$ sample transitions.

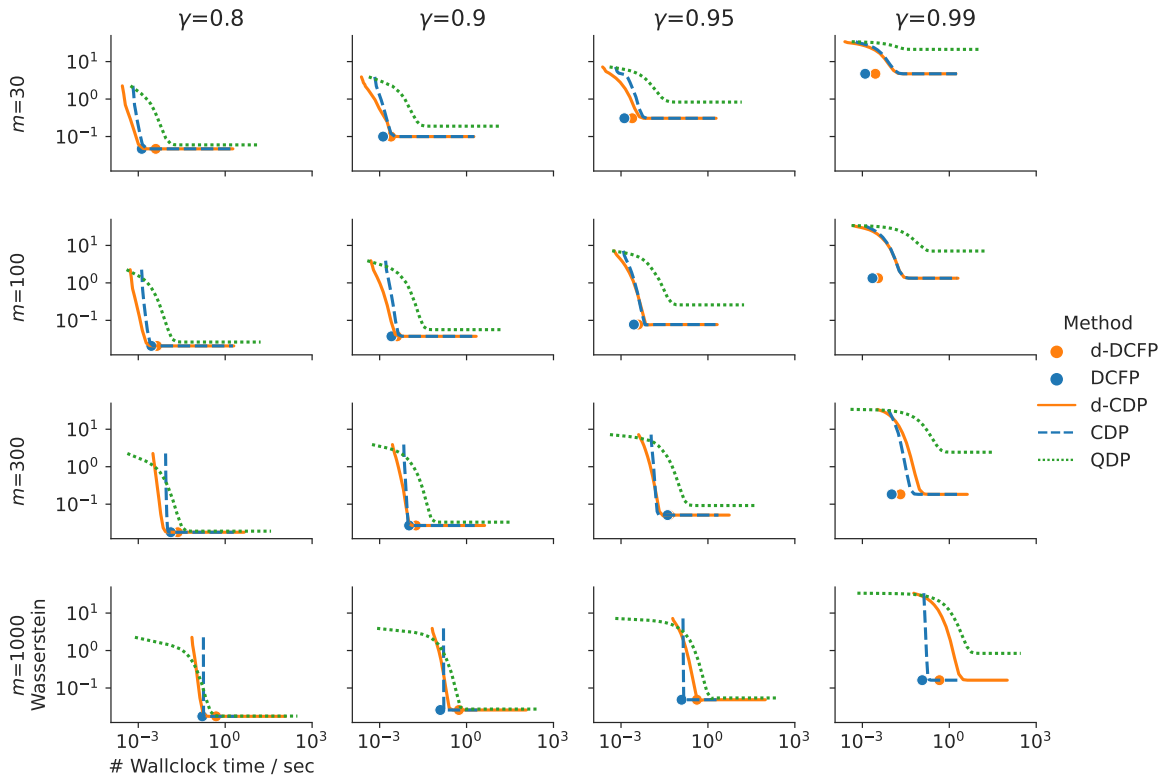
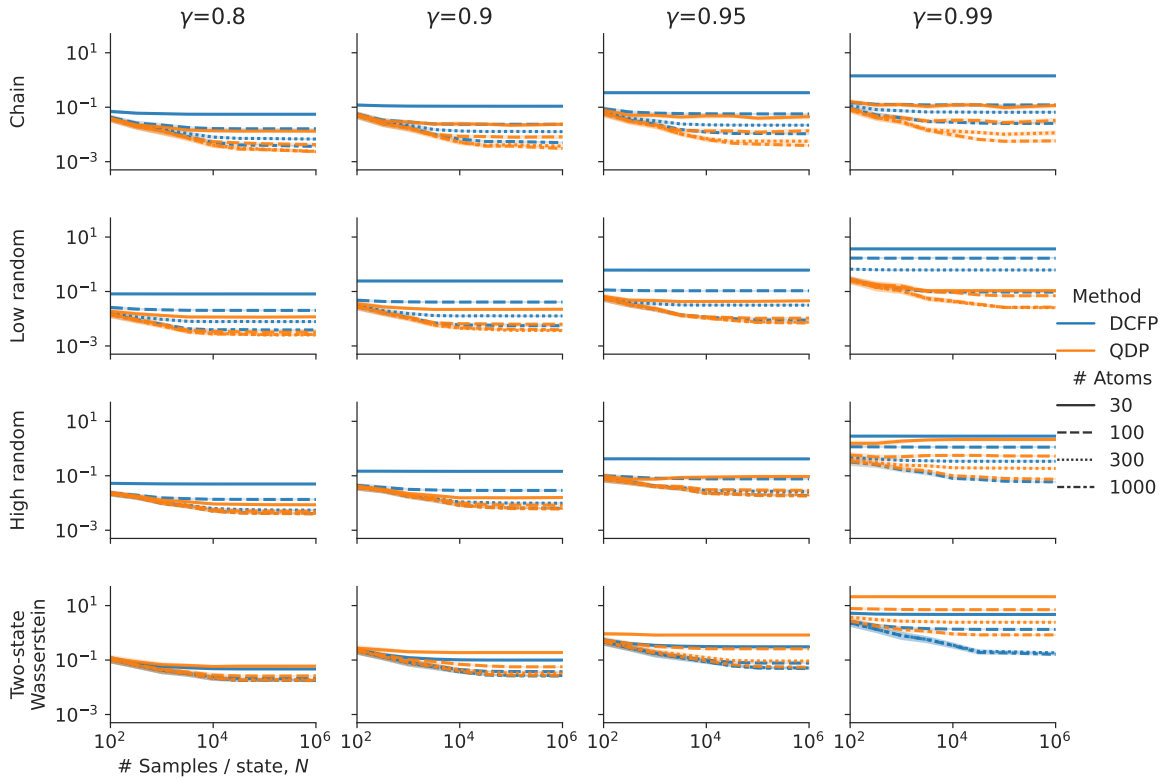
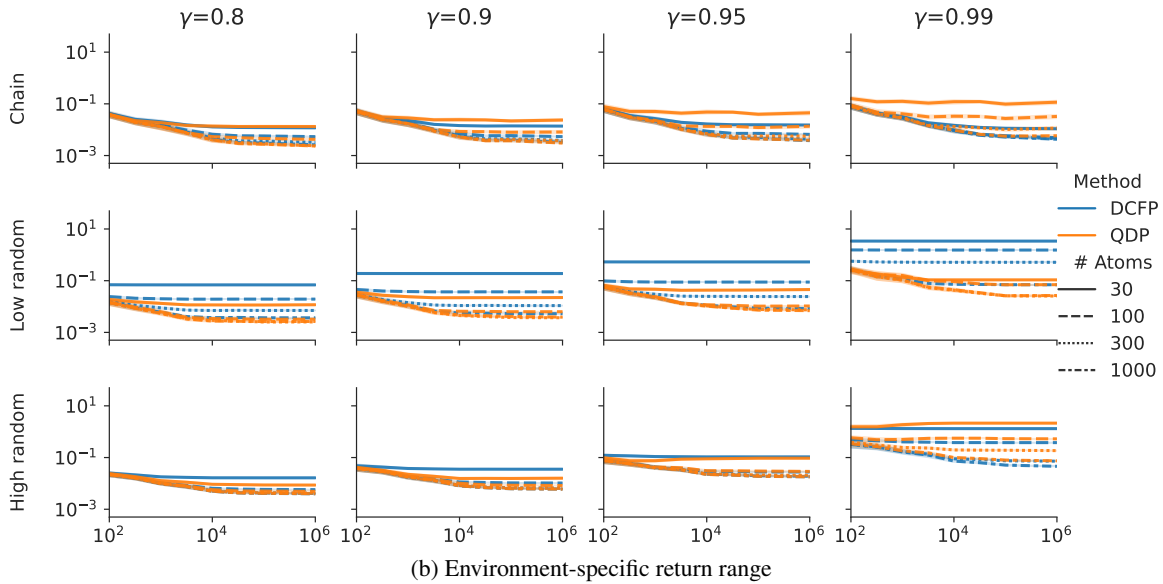


Figure 9. Distance vs. run time results for the two-state environment, for \hat{P} estimated from $N = 10^6$ sample transitions. The return range of this environment coincides with the global return range.



(a) Global return range



(b) Environment-specific return range

Figure 10. Supremum-Wasserstein distance on convergence. Error envelope indicates 95% confidence interval by bootstrapping. The return range of the two-state environment coincides with the global return range.